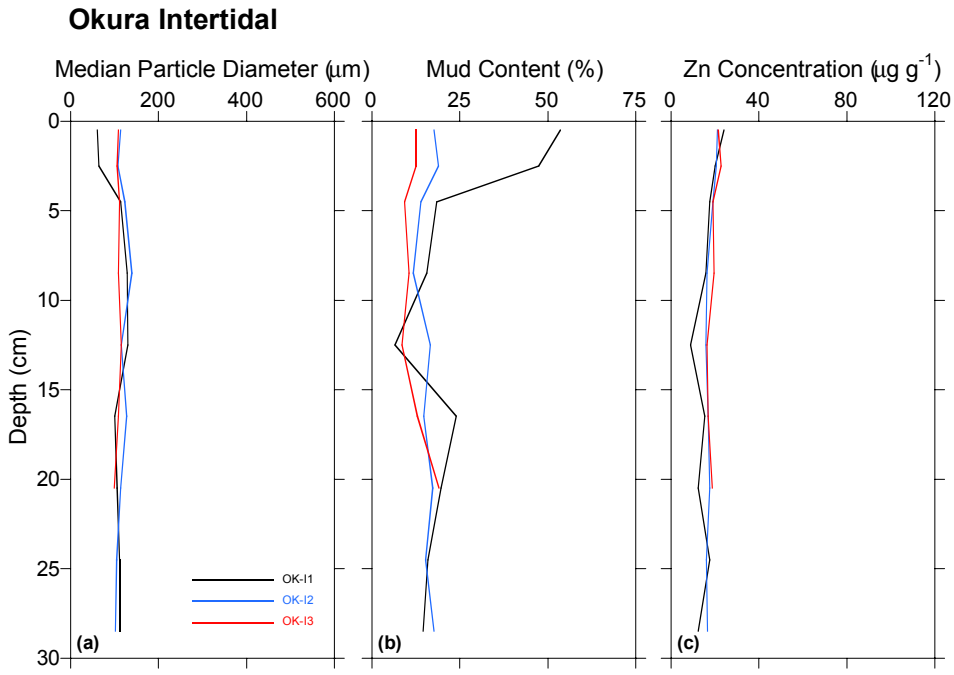

Figure 3.21: Okura intertidal cores (a) median particle diameter, (b) mud content and (c) Zn concentration profiles.

3.4.3 Okura recent sedimentation history

Sediments preserved in the Okura cores are likely to include the Maori period of occupation. Pollen profiles in cores OK-I1 (Fig. 3.22) and OK-I3 are similar in that the rise in pine and grass pollens is observed. The influence of Maori on the catchment is indicated by the coincidence of high bracken and native tree pollens. Sediment mixing down the core is also shown by the isolated occurrence of pine pollen at 24 cm depth (Fig. 3.22). By comparison, relatively high pine and grass pollen counts in core OK-I2 bottom sediments indicate more rapid sedimentation at this site. The presence of ^{137}Cs at the base of core OK-I2 also indicates that sedimentation (SAR ≥5.8 mm yr^{-1}) has been more rapid here than in the other two cores (Fig 3.23). Pollen dating indicates that SAR have increased three-fold from 1–2 mm yr^{-1} (1950–1980) to ~5–6 mm yr^{-1} (1980–2001). The SAR value of 10.5 mm yr^{-1} for core OK-I2 is substantially higher than the other two cores.

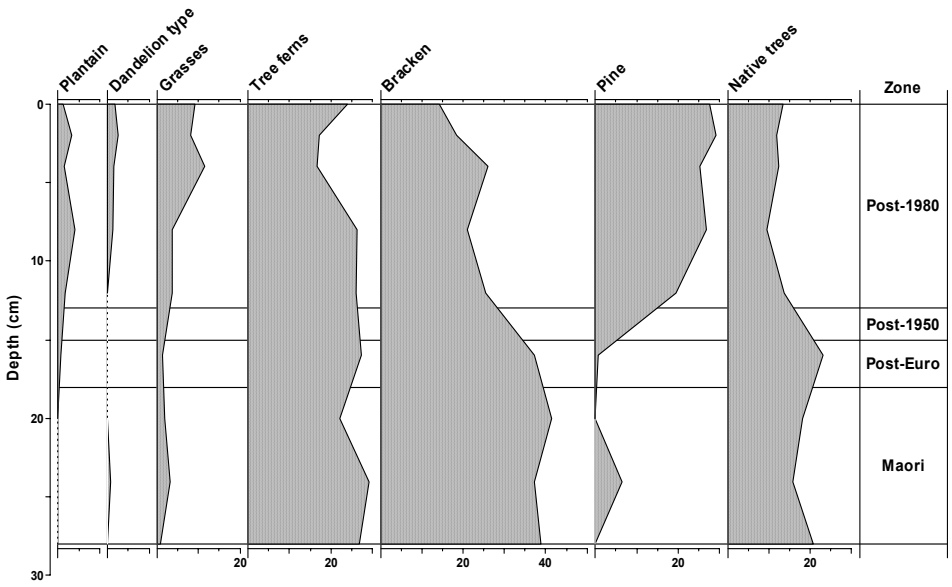

Figure 3.22: Okura estuary intertidal core OK-I1 pollen and spore profiles for major plant groups expressed as percentage of terrestrial pollen and spore sum.

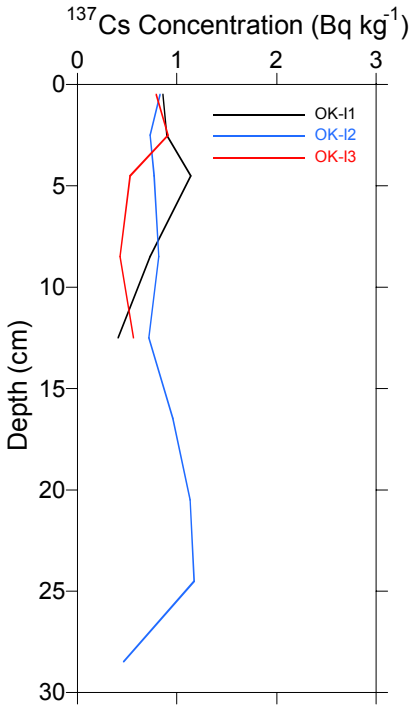

Figure 3.23: ^{137}Cs concentration profiles in the Okura intertidal cores.

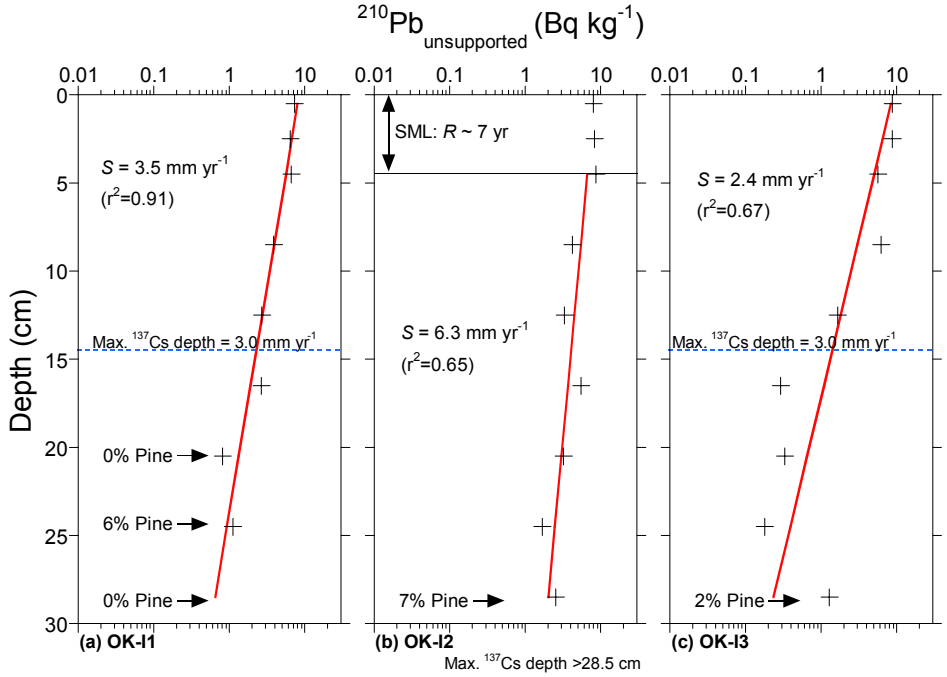

Figure 3.24: Okura intertidal cores. Unsupported ^{210}Pb profiles plotted on a log scale, with linear regression fits used to calculate sedimentation rates (*S*). Also shown are the surface-mixed layer (SML), associated particle residence time (*R*) and the maximum depth of ^{137}Cs and average SAR.

The ^{210}Pb profiles also show that sedimentation has been more rapid in core OK-I2 than in the other two cores (Fig. 3.24). The ^{210}Pb-derived SAR of 6.3 mm yr^{-1} is similar to the minimum ^{137}Cs value of ≥5.8 mm yr^{-1}. The uniform ^{210}Pb concentrations in the top 5 cm of core OK-I2 is indicative of a surface mixed with a particle residence time of ~7 years. Comparison of SAR for the historical time-periods highlights the differences between core OK-I2 and cores OK-I1 and OK-I3 (Fig. 3.25). The substantially higher SAR observed in OK-I2 is probably due to sediment mixing as shown by its pollen (Appendix II) and ^{210}Pb profiles. Cores OK-I1 and OK-I3 have similar pollen (3.1–3.4 mm yr^{-1}), ^{210}Pb (2.4–3.5 mm yr^{-1}) and ^{137}Cs SAR (3.0 mm yr^{-1}) for the post-1950/1953 period, which provides a high degree of confidence in these results.

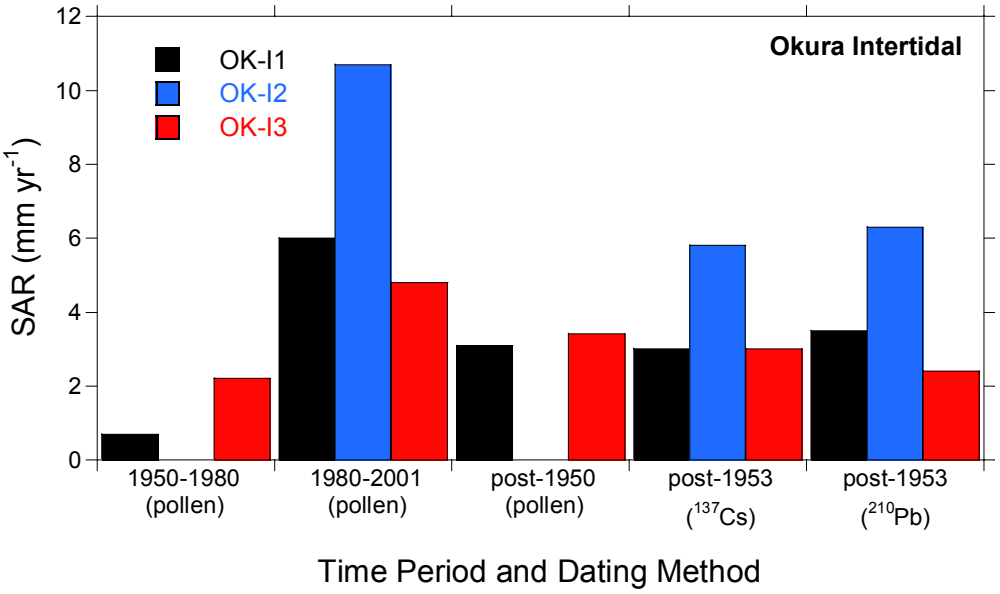

Figure 3.25: Okura intertidal cores, comparison of SAR estimated from pollen, ^{137}Cs and ^{210}Pb dating.

Close agreement between the dating methods and good linear regression fits to the ^{210}Pb data for cores OK-I1 and OK-I3 enable us to reconstruct changes in SAR during the last ~150 years using the constrained ^{210}Pb CRS dating model (Figs. 3.26 & 3.27). We calculate depth-age, age-mass sedimentation (g cm^{-2} yr^{-1}) and age-SAR (mm yr^{-1}) curves for three depth increments. This accounts for the uncertainty in the maximum depth of ^{137}Cs ($^{137}Cs_{max}$), which results from the 4-cm depth interval between samples.

The depth-age estimates for core OK-I1 show the effect of differences in maximum ^{137}Cs depth on the ^{210}Pb CRS model as well as differences between the CRS and CIC model (Fig. 3.26a). There is good agreement between the CRS curves for sediments <50 years old and between the CRS 16.5-cm (depth) ^{137}Cs and CIC models. Blais et al. (1995) found that age discrepancies between the CRS and CIC models can be expected where sedimentation rates have substantially increased in the last 150 years or so. The age-mass sedimentation curves show a four-fold increase from ~0.1 g cm^{-2} yr^{-1} 100–150 years ago to ~0.4 g cm^{-2} yr^{-1} to the present day (Fig. 3.26b). Similarly, the age-SAR curves indicate that net sedimentation rates have increased from pre-deforestation values of ~0.5 mm yr^{-1} to ~3.5 mm yr^{-1} today (Fig. 3.26c).

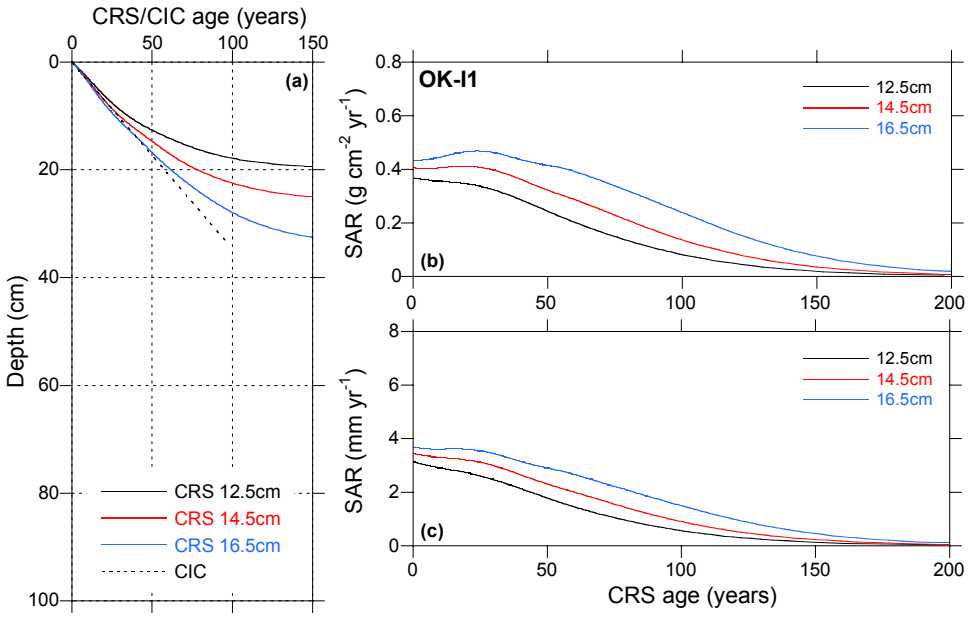

Figure 3.26: Core OK-I1 sedimentation chronology (a) depth-age curves for CRS and CIC ^{210}Pb models, (b) age-mass (g cm^{-2} yr^{-1}) accumulation curves and (c) age-SAR (mm yr^{-1}) curves based on the constrained CRS model. Note: we calculate curves for three depth increments to account for the uncertainty in the maximum depth of ^{137}Cs ($^{137}Cs_{max}$), which results from the 4-cm depth interval between samples.

Table 3.2 summarises the constrained ^{210}Pb CRS modelling results for core OK-I1. It can be seen that the depth for integration of the unsupported ^{210}Pb profile to satisfy Equations 4 and 5 increases with $^{137}Cs_{max}$. The total unsupported ^{210}Pb in the sediment column ($A(o)$) and the mean annual atmospheric ^{210}Pb flux (P) estimated from the core is relatively insensitive to changes in $^{137}Cs_{max}$. This is primarily because the unsupported ^{210}Pb concentration decreases exponentially with depth in the sediment column.

Table 3.2: Summary of constrained ^{210}Pb CRS modelling results for core OK-I1: linear regression fit to natural-log transformed ^{210}Pb data; depth for integration of ^{210}Pb profile; total unsupported ^{210}Pb in the profile ($A(o)$) and mean annual flux (P).

	$^{137}Cs_{max}$ = 12.5 cm	$^{137}Cs_{max}$ = 14.5 cm	$^{137}Cs_{max}$ = 16.5 cm
^{210}Pb profile fit (r^2)	0.91	–	–
^{210}Pb profile depth (cm)	19.8	25.8	34.1
***A*(*o*)** (Bq cm^{-2})	0.1002	0.1024	0.1178
P (Bq cm^{-2} yr^{-1})	0.0031	0.0034	0.0037

An important test to validate our results is to compare P estimated from core OK-I1 with direct measurements of the atmospheric flux. P values for core OK-I1 (0.0031–0.0037 Bq cm^{-2} yr^{-1}) are of the same order as the 0.0059 Bq cm^{-2} yr^{-1} measured in rainfall at Mangemangeroa during 2002–2003. At Hokitika, the standard deviation of P (0.0019 Bq cm^{-2} yr^{-1}) in rainfall (1995–2000) represents 15% of the 0.0117 Bq cm^{-2} yr^{-1} average value (section 2.2.2). Given this inter-annual variability in P, we conclude that there is no substantial difference between our P estimates for core OK-I1 and P measured directly in Auckland rainfall.

The same analysis was carried out on core OK-I3 (Fig. 3.27). Results are only available for the $^{137}Cs_{max}$=12.5-cm case because there is insufficient unsupported ^{210}Pb in the profile below that depth to satisfy Equation 4. There is close agreement between the CRS and CIC model depth-age curves for sediments <100 years old (Fig. 3.27a). The age-mass sedimentation curve shows an increase from ~0.1 g cm^{-2} yr^{-1} 150 years ago to a maximum of 0.36 g cm^{-2} yr^{-1} in the mid-1960's (CRS age 37 years) and followed by a small decrease since that time (Fig. 3.27b). The age-SAR curve follows a similar pattern, with SAR increasing from <1 mm yr^{-1} 150 years ago to 2.5 mm yr^{-1} today (Fig. 3.27c).

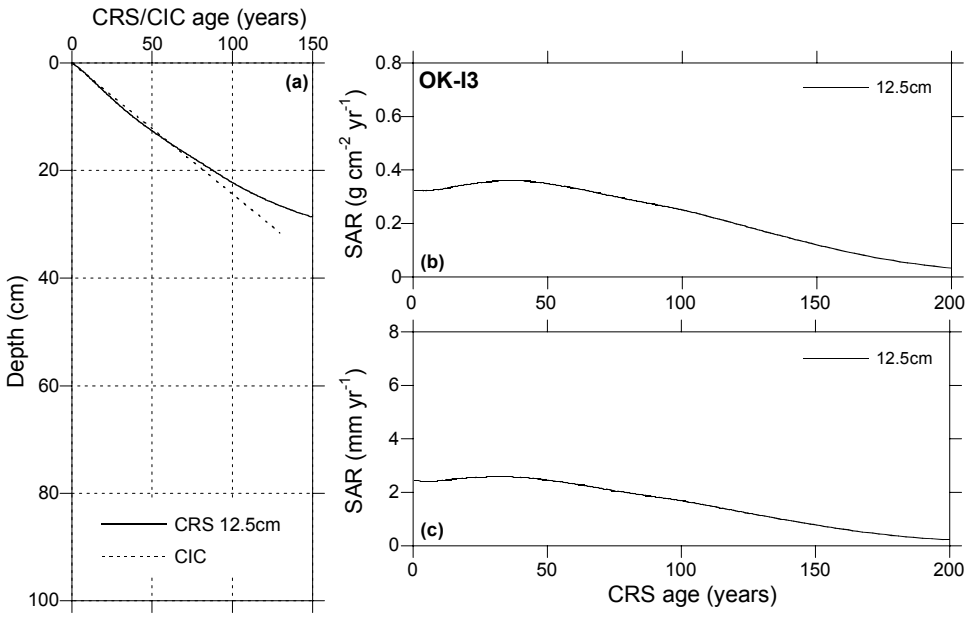

Figure 3.27: Core OK-I3 sedimentation chronology (a) depth-age curves for CRS and CIC ^{210}Pb models, (b) age-mass (g cm^{-2} yr^{-1}) accumulation curves and (c) age-SAR (mm yr^{-1}) curves based on the constrained CRS model.

The apparent peak in SAR ~37 years ago could coincide with planting of the adjacent pine forest at Wieti Station in the early 1970's. However, the absence of a similar peak in core OK-I1 suggests that the apparent peak is a result of local sediment dynamics and/or sediment bulk density variation rather than a period of increased catchment soil erosion. Table 3.3 summarises the constrained ^{210}Pb CRS modelling results for core OK-I3. The $A(o)$ and P values for core OK-I3 are very similar to core OK-I1 (Table 3.2). This between-core consistency provides confidence in the sedimentation histories reconstructed for both cores.

Table 3.3: Summary of constrained ^{210}Pb CRS modelling results for core OK-I3: linear regression fit to natural-log transformed ^{210}Pb data; depth for integration of ^{210}Pb profile; total unsupported ^{210}Pb in the profile ($A(o)$) and mean annual flux (P).

	$^{137}Cs_{max}$ = 12.5 cm
^{210}Pb profile fit (r^2)	0.67
^{210}Pb profile depth (cm)	31.7
***A*(*o*)** (Bq cm^{-2})	0.0948
P (Bq cm^{-2} yr^{-1})	0.0030

3.5 Henderson creek (intertidal cores)

3.5.1 Background

Henderson Creek is a tributary drowned-valley estuary of the Waitemata Harbour (Fig. 3.28). The estuary has a high-tide surface area of ~2.0 km^2 and is sheltered from the harbour proper by the Te Atutu Peninsula. Henderson Creek has infilled with sediment and in its upper reaches, mangrove has entirely colonised the intertidal flat. At the mouth of the estuary, an extensive intertidal flat has accreted, which is also extensively colonised by mangrove. The estuary receives runoff from a 105.1-km^2 catchment.

The catchment landcover history of the Waitakere ranges is described by Denyer et al. (1993). The original native forest of the Waitakere ranges consisted of an undisturbed, mixed conifer-hardwood forest dominated by kauri, rata, toatoa and rimu with tree ferns. Large-scale deforestation of Henderson catchment began in 1849, when Thomas Henderson and John Macfarlane began logging kauri timber. Between 1849–1864 an estimated 45 million feet of timber was cut at Dundee Sawmills, Henderson (Graeme Murdoch, ARC Director - Natural Heritage, pers. comm. 2002). By the late 1860's almost the entire Henderson estuary catchment had been deforested.

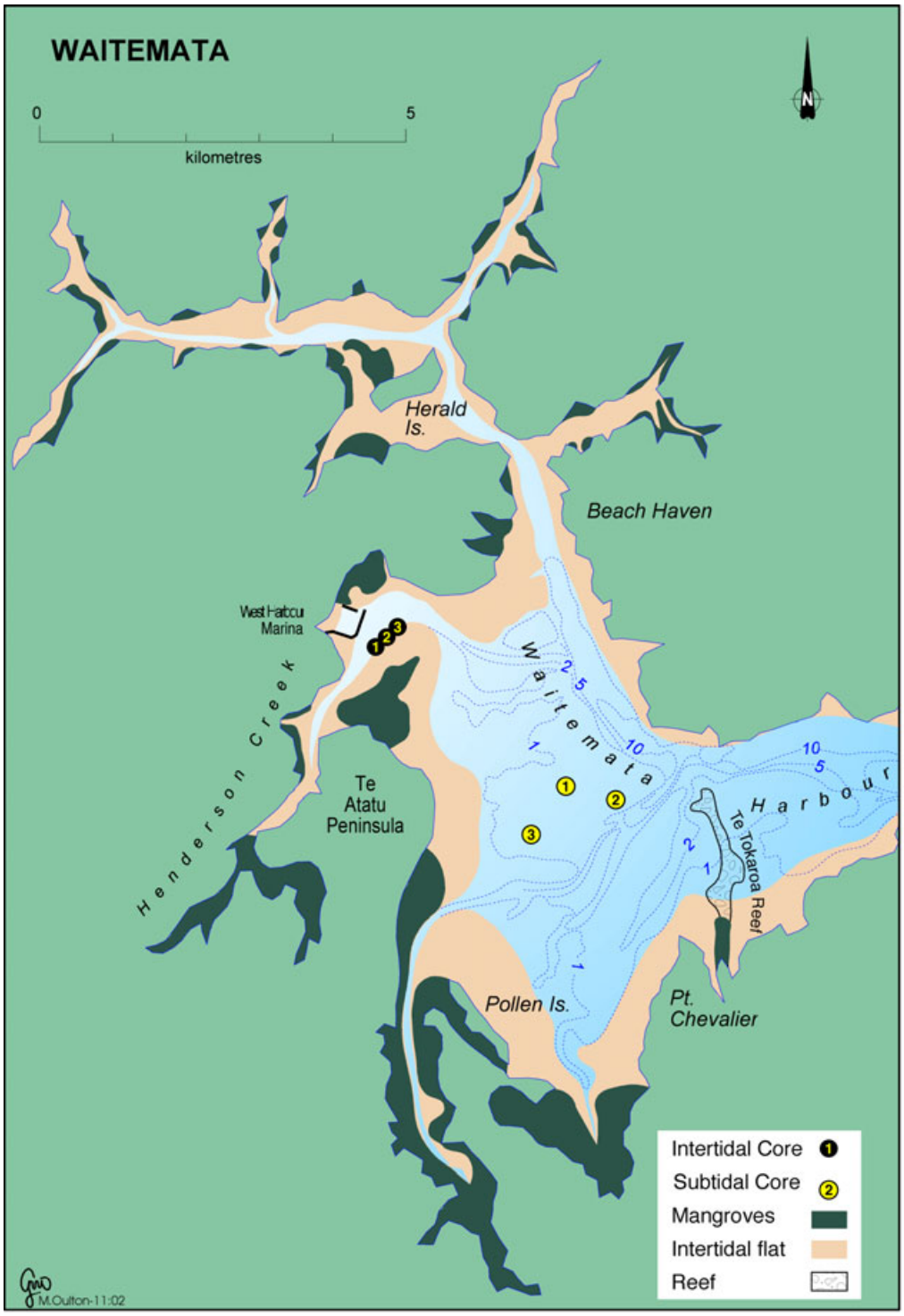

Figure 3.28: Waitemata harbour - location of intertidal (Henderson) and sub-tidal (Te Atatu) and cores and major sub-environments.

Most of the Henderson Valley was deforested, with the exception of the steep and inaccessible upper reaches of the sub-catchments. The process of establishing pasture involved clearing native scrub by fire, which often burnt out of control (Denyer et al. 1993). It is likely that catchment soil erosion increased during this period. In the 1890's viticulture and orcharding was established in the lower catchment and Henderson township was growing. By the 1920's, farming had virtually ceased because of soil infertility and poor road access. Large-scale urban development began in the late 1950's, following the development of the north-western motorway at Henderson whereas urban development at Massey and on the Te Atatu Peninsula began in the 1970's. Present day catchment landcover is comprised of regenerating native forest (49%) and scrub (5%), urban (21%) and pasture (25%) (source: NZ Land Resource Inventory). Today native forest is regenerating in the upper reaches of the catchment.

3.5.2 Henderson estuary sediments

Replicate sediment cores were collected from a large intertidal mud bank at the mouth of Henderson Creek and opposite the West Harbour Marina in Limeburners Bay. Figure 3.29 shows a view southeast from site two across the middle harbour towards Auckland city. The core sites were ~100-m apart and parallel to the main tidal channel (Fig. 3.28). Core sediments are mixtures of fine silt (~20 μm modal diameter) and very fine sand (~100–150 μm modal diameter). Dry bulk sediment densities (0.9–1.5 g cm^{-3}) are similar in all cores and relatively uniform with depth (Appendix III). Profiles of D_{50} are similar in all three cores and show negligible variation between sites or with depth in the sediment column. Median particle diameters range between 120–190 μm (Fig. 3.30a). The profiles of sediment mud content also only show small variations between sites and vary between 5–12% (Fig. 3.30b).

Zn profiles for the Henderson cores are similar and show that Zn concentrations consistently increase towards the sediment surface (Fig. 3.30c). The Zn concentrations at the base of cores (28–53 μg g^{-1}) exceed the pre-urban "background" range of 10–30 μg g^{-1} typical of Auckland estuaries. This suggests that sediments at the base (28–29 cm depth) of the cores were deposited during the period of urban development. Zn concentrations at the surface vary between 83–100 μg g^{-1}.

Figure 3.29: Henderson estuary, view from HN-I3 looking southeast across the middle Waitemata harbour towards Auckland city.

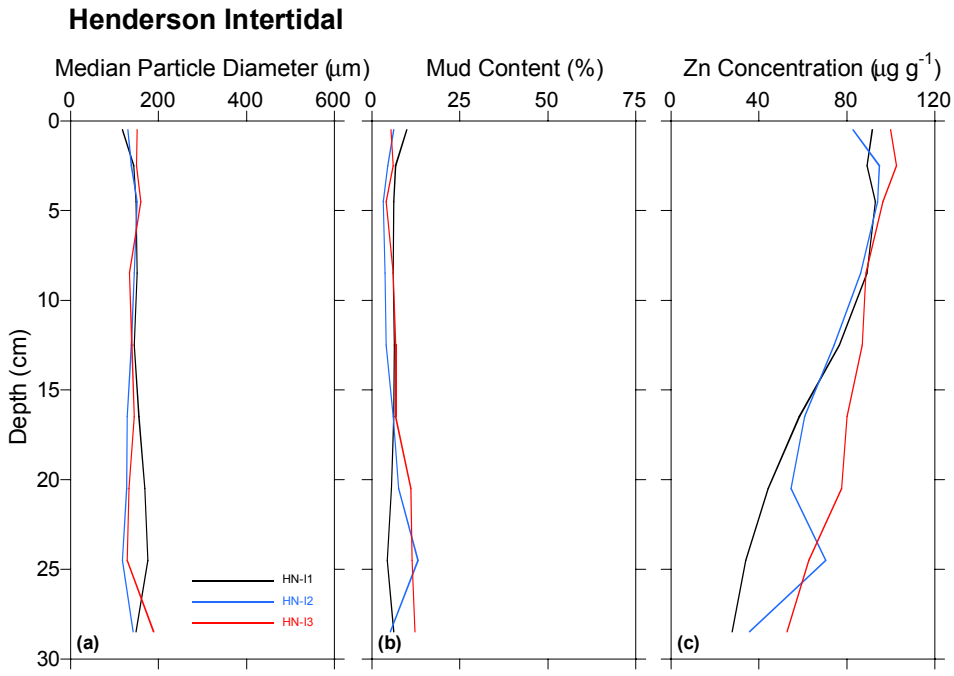

Figure 3.30: Henderson intertidal cores (a) median particle diameter, (b) mud content and (c) Zn concentration profiles.

3.5.3 Henderson creek recent sedimentation history

The pollen records in the Henderson cores are difficult to interpret because of the relatively low number of samples analysed. Figure 3.31 shows the pollen profiles for core HN-I2. Pine is present at the base of all the Henderson cores, which indicates that the upper ~0.3 m of the sediment column has been deposited since the mid-1930's and/or sediment mixing has transported pollen down the profile. Analysis of samples at intermediate depths would likely improve the resolution, and thus interpretation of these pollen profiles. Although the rise in pine and grass pollens is observed in these cores, there are high levels of native tree pollen, which is likely to reflect the fact that the estuary catchment includes regenerating native forest of the Waitakere Ranges. The fact that Zn concentrations in basal sediments (28–53 μg g^{-1}) exceed pre-urban "background" values is consistent with urban development from the early 1900's.

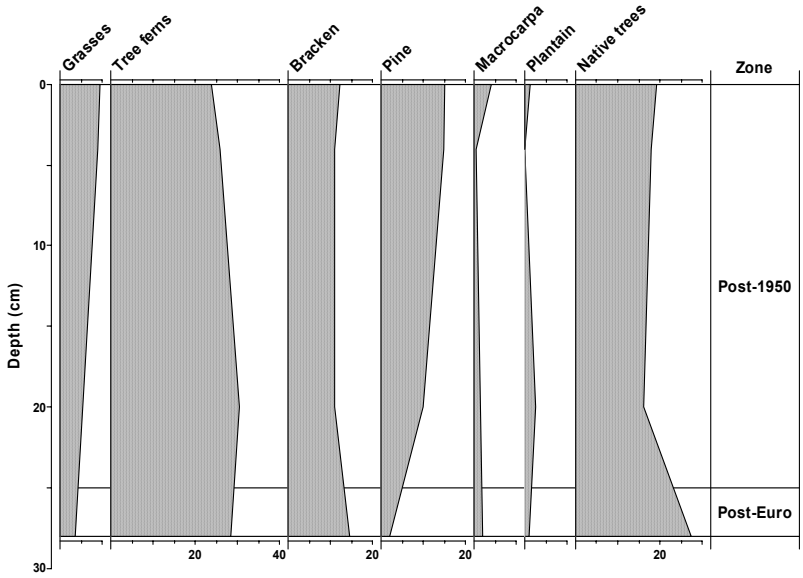

Figure 3.31: Henderson creek intertidal core HN-I2 pollen and spore profiles for major plant groups expressed as percentage of terrestrial pollen and spore sum.

The presence of ^{137}Cs at the sediment surface indicates that these sediments are derived from eroded catchment soils (Fig 3.32) as atmospheric deposition ^{137}Cs has not been detected in New Zealand since the mid-1980's. Also, the presence of ^{137}Cs at the bottom of core HN-I3 suggests more rapid sedimentation and/or sediment mixing at this site in comparison with cores HN-I1 and HN-I3.

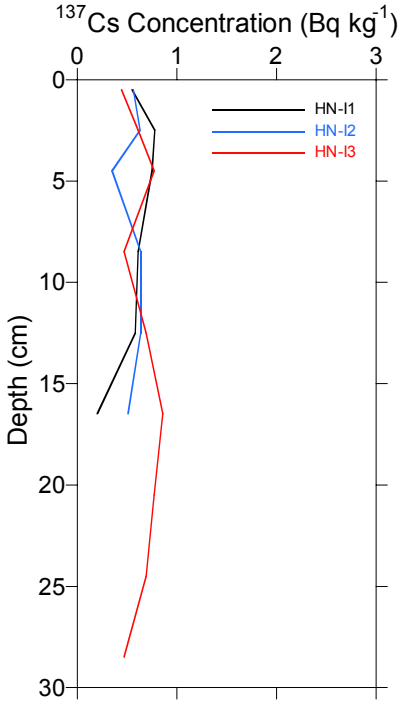

Figure 3.32: ^{137}Cs concentration profiles in the Henderson intertidal cores.

The ^{210}Pb profiles display uniform ^{210}Pb concentrations in the top 2.5–5 cm of the sediment column, which we interpret as surface-mixed layers (Fig. 3.33). The ^{210}Pb-derived SAR of 2.6–3.2 mm yr^{-1} in cores HN-I1 and HN-I2 are similar to ^{137}Cs SAR (3.8 mm yr^{-1}) for the post-1953 period (3.34). The substantially steeper ^{210}Pb profile in core HN-I3 results in a higher SAR (5.1 mm yr^{-1}), which is similar to the minimum ^{137}Cs value of ≥5.8 mm yr^{-1}. We estimate particle residence times in the SML of between 5–14 years based on the ^{210}Pb-derived SAR.

The lack of resolution in the pollen profiles does not enable the post-1950 and post-1980 to be distinguished in all the cores. We have tentatively interpreted the presence of high concentrations of pine pollen at depth in core HN-I1 as evidence of increased sedimentation (~6 mm yr^{-1}) since the early 1980's (Fig 3.34). However, we have no independent dating to confirm this interpretation.

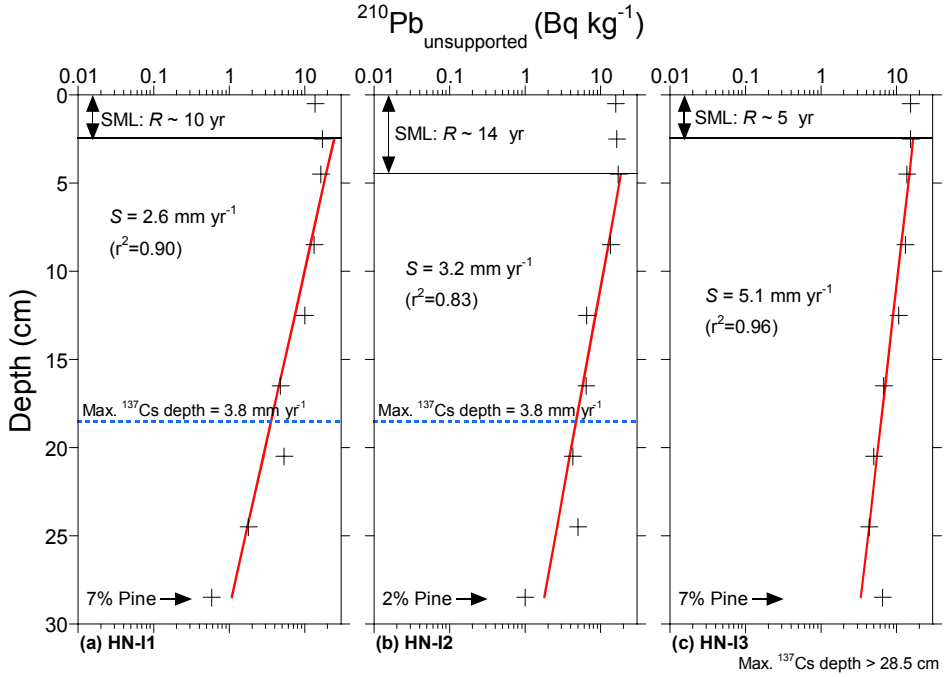

Figure 3.33: Henderson intertidal cores. Unsupported ^{210}Pb profiles plotted on a log scale, with linear regression fits used to calculate sedimentation rates (*S*). Also shown are the surface-mixed layer (SML), associated particle residence time (*R*) and the maximum depth of ^{137}Cs and average SAR.

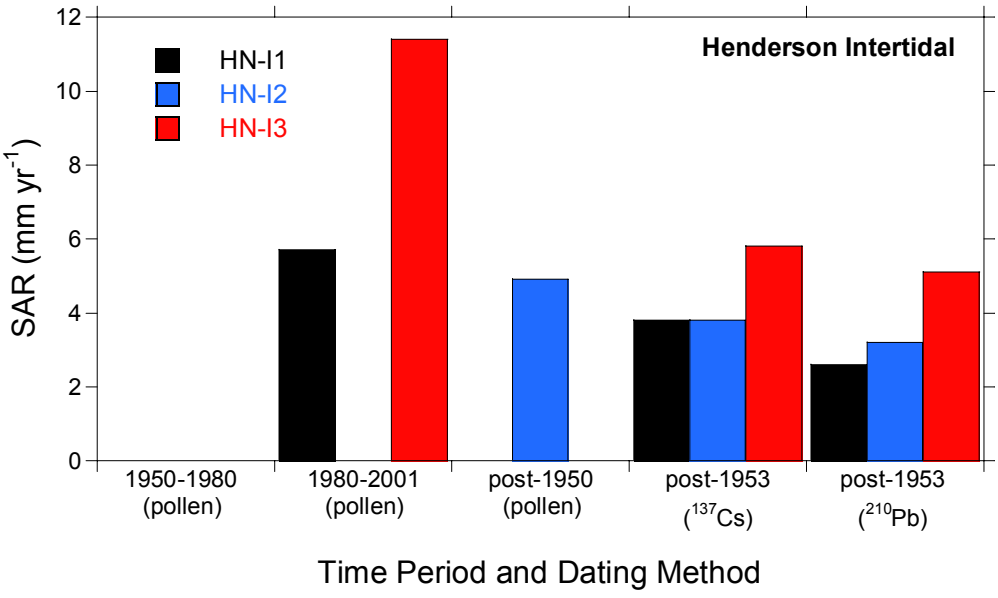

Figure 3.34: Henderson intertidal cores, comparison of SAR estimated from pollen, ^{137}Cs and ^{210}Pb dating.

3.6 Waitemata-Te Atatu (sub-tidal cores)

3.6.1 Background

The Waitemata Harbour is the largest estuary on Auckland's east coast (Fig. 3.28). The estuary has a surface area of 80 km^2 and a tidal prism (~216 million m^3) which is five times larger than the Mahurangi estuary, which is the next largest east coast estuary (Table 3.1). The Waitemata is a drowned valley, which remains largely sub-tidal except in the numerous infilled tidal creeks, which fringe the estuary. The middle estuary between Te Atatu Peninsula and the Auckland Harbour Bridge is a shallow subtidal basin with water depths typically < 2 m below chart datum (Fig. 3.28). The extensive sub-tidal flat east of Te Atatu Peninsula is dissected by channels which drain the upper harbour, Henderson and Whau Creeks. The subtidal flat gradually shoals west towards the Te Atatu Peninsula, which is fringed by a 0.5–1-km wide intertidal flat. The Waitemata receives runoff from a 427-km^2 catchment, which includes large areas of Auckland City, North Shore, Albany and West Auckland.

The early-European catchment landcover history of the Upper Waitemata Harbour is previously discussed (section 3.5.1). Auckland City developed from the 1840's and by the early 1900's land fringing the southern shore of middle harbour, such as Avondale, Point Chevalier and Herne Bay, had been urbanised. However, large-scale urbanisation of the North Shore did not occur until the completion of the Auckland Harbour Bridge in the early-1950's. Prior to this, catchment landcover was mainly native scrub and pasture. For example, urbanisation of Hellyers Catchment began immediately after the harbour bridge construction and by the early-1970's was largely complete (Williamson and Morrisey, 2000). By comparison, many of the catchments draining to the Upper Waitemata Harbour, including Lucas, Paremoremo and Rangitopuni remain predominantly rural today. Planting of the ~5000 ha Riverhead forest began in 1927 and was completed by the early 1930's. Several pine species were trialed, however growth of the first rotation was slow because of a soil phosphate deficiency, which was not recognised until the 1950's. Subsequently, Riverhead Forest was planted with *P. radiata* (Lamb, 2001).

3.6.2 Waitemata sub-tidal sediments

Replicate sediment cores were collected ~1 km apart from the sub-tidal flat east of Te Atutu Peninsula bounded by the tidal channels draining the Henderson and Whau Creeks (Fig. 3.28). Here, sub-tidal sediments are typically muddy fine sands

composed of fine silt (~20 μm modal diameter) and very fine sand (~100–150 μm modal diameter). However, at core site WT-S1 sediments below 5-cm are composed of slightly muddy fine–coarse sands. Dry bulk sediment densities below 12-cm depth in all cores are lower and more variable (0.6–1.8 g cm^{-3}) than above 12-cm depth (1.2–1.7 g cm^{-3}, Appendix III). These density profiles do not conform to the usual pattern of increasing density with depth due to compaction and de-watering.

Profiles of D_{50} for the Te Atatu subtidal cores show large variations between sites. At site WT-S1 the median particle diameter below 20-cm depth is ~530 μm (i.e., medium sand) and abruptly reduces to fine sand above this depth (Fig. 3.35a). At site WT-S2, depth variations in the D_{50} (~150 μm) are negligible, whereas at site WT-S3 median particle size gradually increases from ~30 μm (fine silt) at the base of the core to ~120 μm (very fine sand) at the surface. The mud content profiles are similarly complex, with large variations between core sites, particularly in the lower half of the cores where mud content varies between 5–50% (Fig. 3.35b). By comparison the profiles above 15-cm depth show much less variation (mud content 5-10%).

The Zn concentration profiles measured in the Te Atutu sub-tidal cores (Fig. 3.35c) are very similar to those measured in the Henderson Creek intertidal cores. The Zn concentrations at the base of cores (27–47 μg g^{-1}) generally exceed the pre-urban "background" range of 10–30 μg g^{-1} and, like the Henderson cores, indicate that basal sediments were deposited during the period of urban development. Zn concentrations at the surface vary between 95–105 μg g^{-1}. These results indicate Zn contamination of sediments over a large area of the middle-harbour sub-tidal flats.

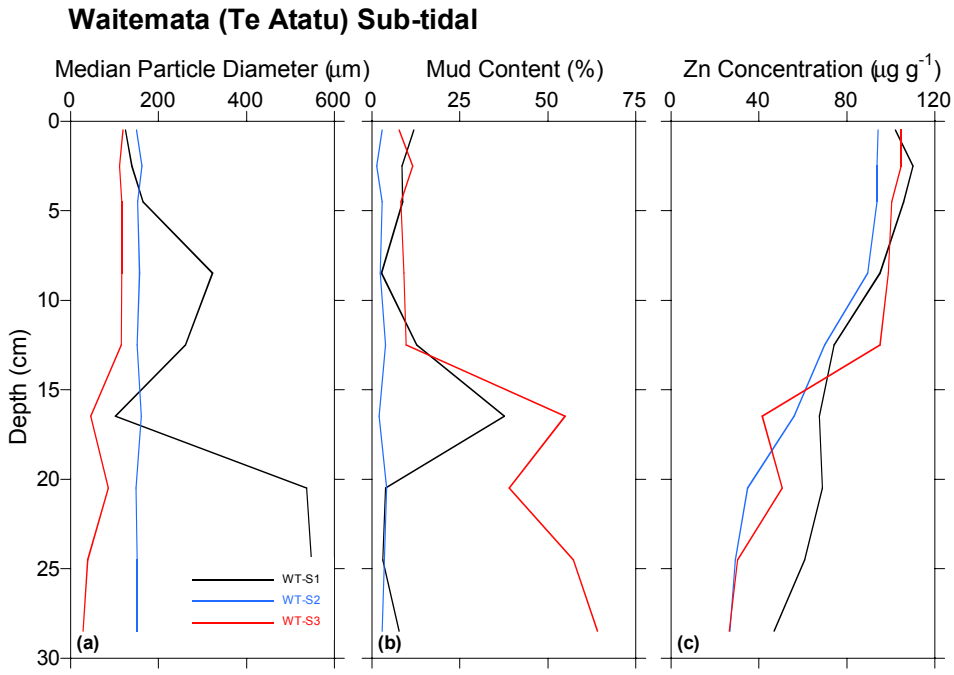

Figure 3.35: Waitemata (Te Atatu) subtidal cores (a) median particle diameter, (b) mud content and (c) Zn concentration profiles.

3.6.3 Waitemata (sub-tidal) recent sedimentation history

The absence of pine pollen at the base of the Waitemata sub-tidal cores indicates that the top-most ~30 cm of the sediment column have been deposited since the early 1900's (Fig. 3.36). The relatively high native tree pollen content of the cores likely reflects the close proximity of the Waitakere ranges, where native forest has been regenerating since the early 1900's. Furthermore, the elevation of the ranges and the prevailing south-westerly wind would favour native pollen input via direct atmospheric deposition, as well as incorporated in eroded soils, to the Waitemata Harbour. The presence of isolated pine pollen and ^{137}Cs peaks at 20-cm depth in core WT-S3 are indicative of downward mixing of sediments (Appendix II). The maximum depth of ^{137}Cs in the cores is evaluated in light of evidence of downward mixing. Consequently the maximum ^{137}Cs depth is estimated as 14.5 cm in all three cores (Fig. 3.37). The presence of ^{137}Cs at the sediment surface indicates that eroded catchment soils are a source of these sediments.

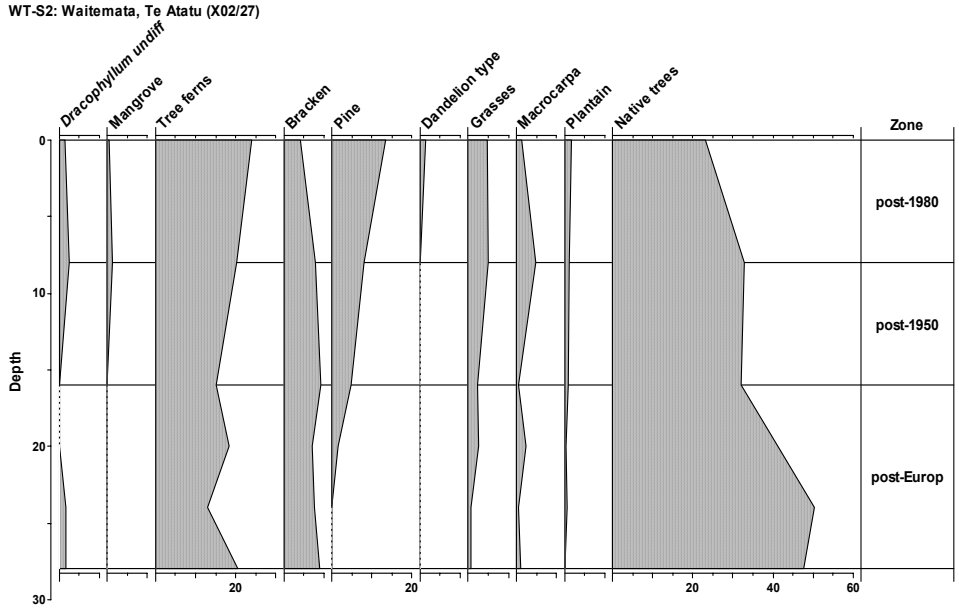

Figure 3.36: Waitemata (Te Atatu) estuary sub-tidal core WT-S1 pollen and spore profiles for major plant groups expressed as percentage of terrestrial pollen and spore sum.

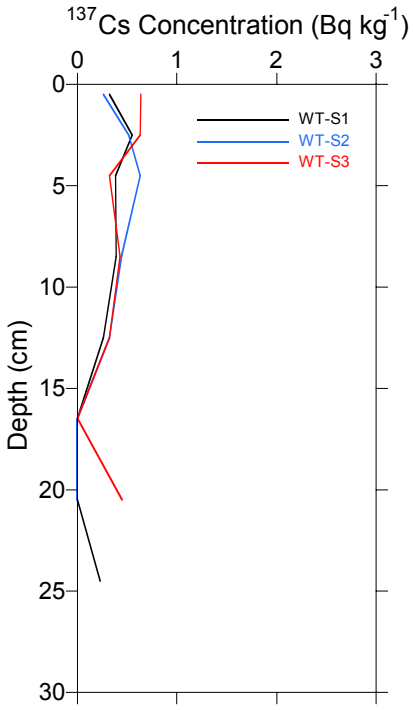

Figure 3.37: ^{137}Cs concentration profiles in the Waitemata (Te Atatu) subtidal cores.

Figure 3.38 shows the ^{210}Pb profiles for the Waitemata subtidal cores. The ^{210}Pb-derived SAR (2.3–3.6 mm yr^{-1}) show between-core consistency and with the ^{137}Cs SAR values (3.0 mm yr^{-1}). The reduced ^{210}Pb concentrations at the surface of cores WT-S2 and WT-S3 are indicative of surface mixing (Fig. 3.38). We estimate particle residence times in the SML of 7 and 11 years based on the ^{210}Pb SAR.

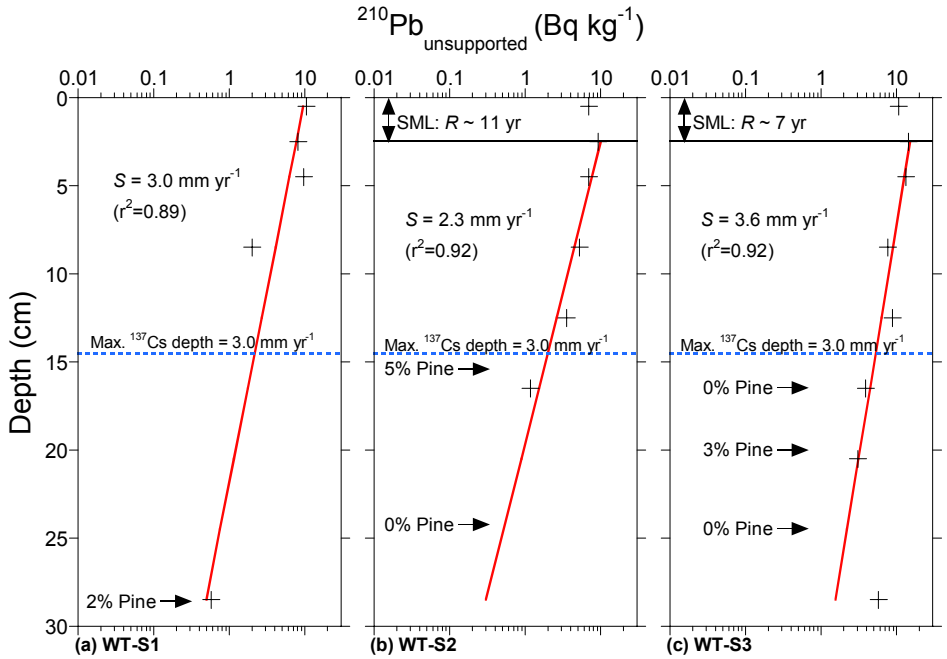

Figure 3.38: Waitemata (Te Atatu) subtidal cores. Unsupported ^{210}Pb profiles plotted on a log scale, with linear regression fits used to calculate sedimentation rates (*S*). Also shown are the surface-mixed layer (SML), associated particle residence time (*R*) and the maximum depth of ^{137}Cs and average SAR.

There is close agreement between SAR derived from pollen, ^{137}Cs and ^{210}Pb CRS dating at all three core sites (Fig 3.39), which provides confidence in these results. These data clearly show that at all sites, net sedimentation rates over the last 50 years have averaged ~3 mm yr^{-1}. Comparison of the pre- and post-1980 pollen data suggests that sedimentation rates in cores WT-S2 and WT-S3 have increased in the last twenty years. We have no independent dating to confirm the pollen result.

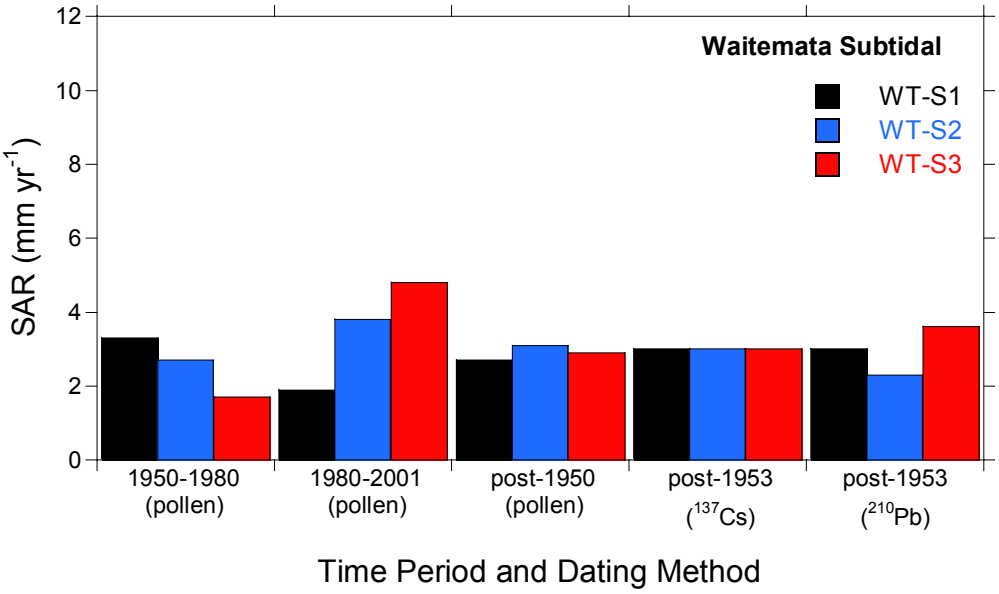

Figure 3.39: Waitemata-Te Atatu (sub-tidal), post-1950/1953 SAR estimated from pollen, ^{137}Cs and ^{210}Pb dating of sediment cores.

3.7 Whitford embayment (sub-tidal cores)

3.7.1 Background

Whitford embayment (11.1 km^2) is an infilled (~80% intertidal) compound estuary on the eastern periphery of the Auckland city (Fig. 3.40, Table 3.1) and receives runoff from a 61-km^2 catchment. The embayment is fringed by the Mangemangeroa, Turanga and Waikopua tidal creeks, which have been infilled with muddy sediments and colonised by mangrove. Analysis of historical aerial photographs shows that the area of intertidal flat occupied by mangrove in the Mangemangeroa and Waikopua tidal creeks has increased by 50% in the last 50 years (Craggs et al. 2001). Furthermore, net sedimentation rates estimated from ^{137}Cs and Zn profiles in sediment cores show that accumulation of these muddy sediments increases towards the heads of these estuaries (Oldman and Swales 1999; Craggs et al. 2001). At the mouth of the Waikopua creek, post-1953 SAR measured in mangrove using ^{137}Cs range from 2.6 to >5.9 mm yr^{-1}, whereas sedimentation rates in the upper reaches of the Mangemangeroa estuary have averaged ~20 mm yr^{-1}. Intensive sediment sampling in the embayment by Gibbs et al. (2001) showed that relatively clay-rich sediments (i.e., 5–10% clay by volume) are accumulating over a large area of

the subtidal compartment offshore from Mellons Bay whereas elsewhere the clay content of surficial sediments is <1%.

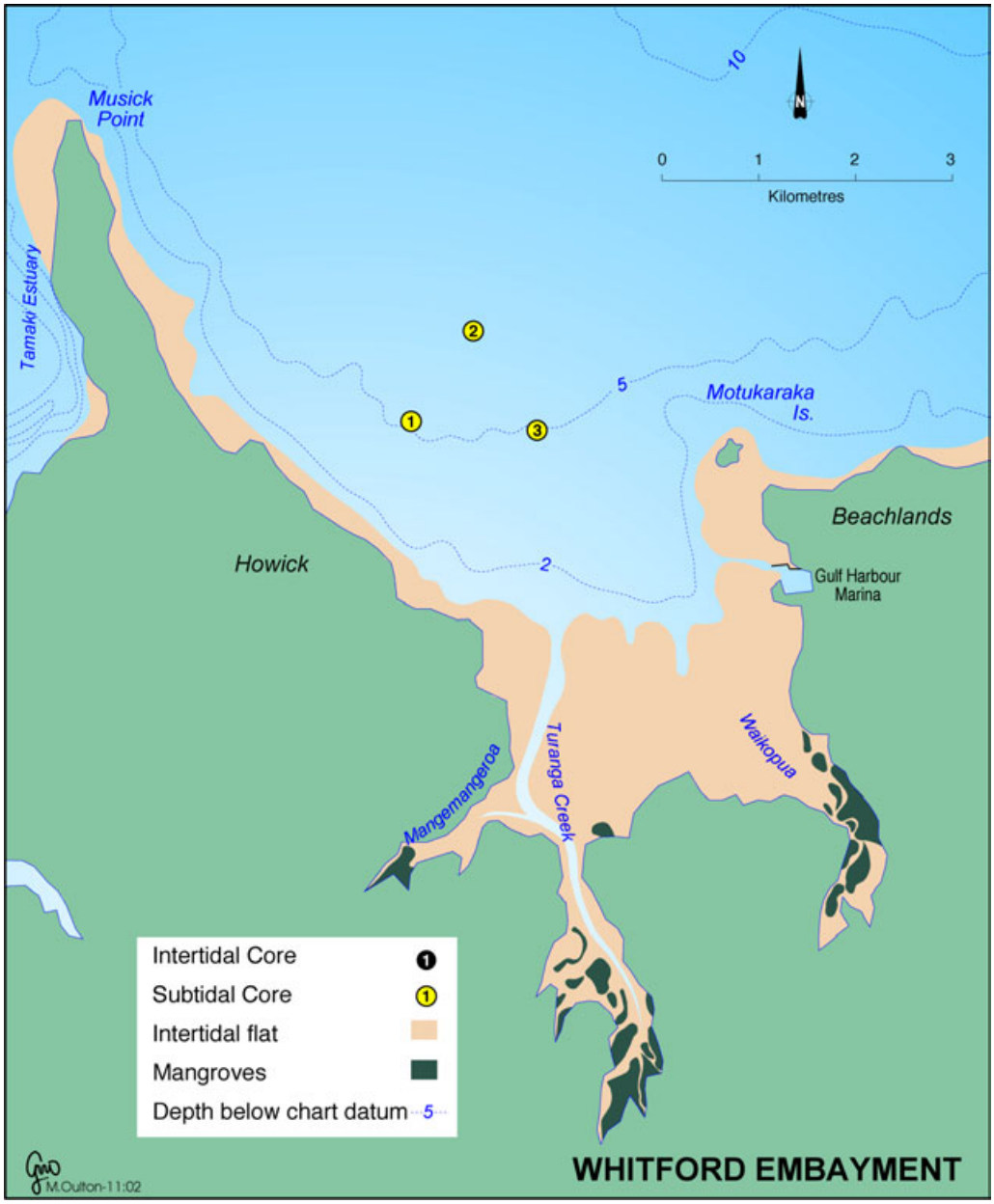

Figure 3.40: Whitford embayment - location of sub-tidal cores and major sub-environments.

The original catchment landcover consisted of an undisturbed coastal forest. Common trees and shrub species included: kohekohe, taraire, hinau, rangiora, kiekie, kawakawa, puriri, karaka, mahoe, pohutakawa, ramarama, putaputaweta, titoki, cabbage tree and tree ferns. The descriptions of early European visitors show that the native forest landcover remained largely intact (Oldman and Swales, 1999). Europeans

first arrived in 1830, although catchment deforestation did not begin until the mid-1840's when the settlement of Howick was established. Owing to the steep terrain in parts of the sub-catchments, such as Mangemangeroa, deforestation was restricted to the ridges and flats above the gullies unlike the neighbouring Pakuranga catchment, which was largely deforested by the early-1900's. Much of the catchment remains relatively undisturbed. Today ~40% of the Mangemangeroa catchment remains under bush/scrub landcover (Morrisey et al. 1999a). This landcover pattern is typical of the entire Whitford catchment.

3.7.2 Whitford sediments

Sediment cores were taken ~1.3 km apart on the subtidal flat east of Mellons Bay in water depths 5–6.5 m below CD (Fig. 3.40) and within the area of clay-rich mud identified by Gibbs et al. (2001). Here, sub-tidal sediments are typically muddy fine sands composed of fine silt (~20 μm modal diameter) and very fine sand (~80–100 μm modal diameter) containing abundant shell valves of *Ruditapes largillierti*, *Austrovenus stuchburyi* (cockle), *Mactra ovata* (mud cockle), *Tellinota edgari* (Tellinid) and oyster. These species are typically found in estuaries and sheltered coastal embayments. In the top ~10 cm of cores WH-S1 and WH-S2 the mud and very fine sand modes are present in roughly equal proportions and below 10 cm depth the mud content of these sediments declines. By comparison in core WH-S3 there is a steady increase in mud content towards the sediment surface. Dry bulk sediment density profiles are similar in all cores (Appendix III) and increase from ~0.5 g cm^{-3} in surface sediments to ~0.9 g cm^{-3} at the base of each core.

Profiles of D_{50} are similar for cores WH-S2 and WH-S3 and show negligible variation with depth (D_{50} range = 60–90 μm). The D_{50} profile for WH-S1 differs from the other two cores below 15-cm depth where median particle size increases to 640 μm, which reflects the fine shell hash content of these sediments (Fig. 3.41a). The cores also show an overall trend of gradually increasing mud content from the bottom (25–35%) to the top (35–55%) of the cores (Fig. 3.41b).

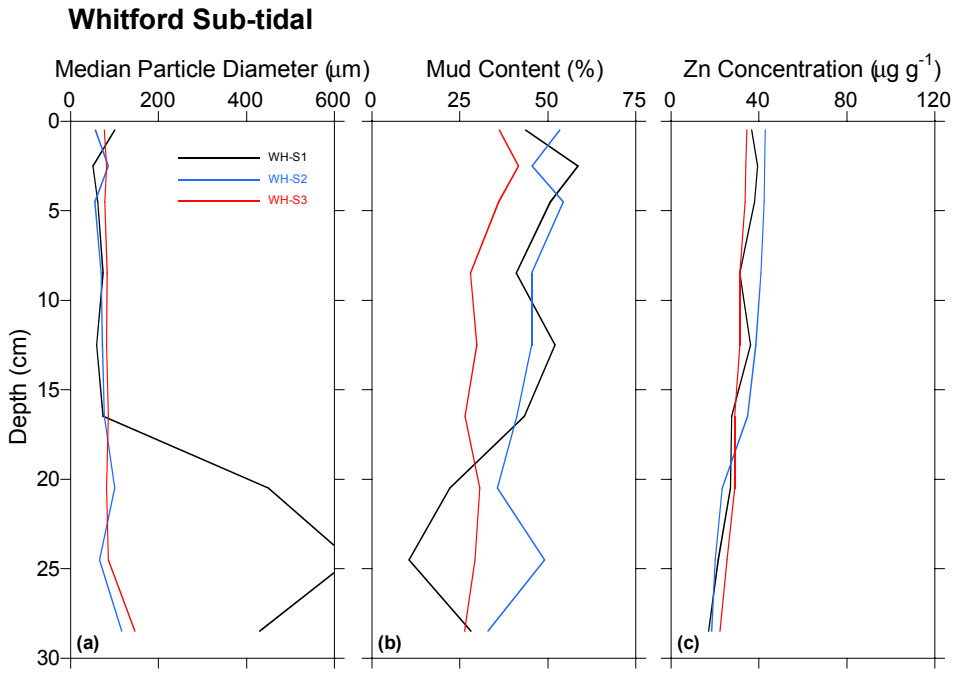

Figure 3.41: Whitford sub-tidal cores (a) median particle diameter, (b) mud content and (c) Zn concentration profiles.

The Zn concentration profiles are similar in each of the Whitford sub-tidal cores (Fig. 3.41c) and show a consistent gradual increase from 17–22 μg g^{-1} in the base of the cores to 35–42 μg g^{-1} at the sediment surface. These data show that Zn concentrations in the subtidal sediments have increased slightly above pre-urban "background" values (i.e., 10–30 μg g^{-1}).

3.7.3 Whitford recent sedimentation history

A clear *P. radiata* pollen signal in all three cores provides confidence in defining the 1950 and 1980 depth horizons. In basal sediments there is a rapid upwards decline in native tree pollen, which marks the latter stages of catchment deforestation (Fig. 3.42). The presence of substantial quantities of native tree pollen in post-1950 sediments reflects the large area of bush remnants that remain in estuary sub-catchments, such as the Mangemangeroa. The ^{137}Cs profiles (Fig. 3.43) are in close agreement with the pollen dating and indicate that the top ~20 cm of sediment has been deposited in the last 50 years. The presence of pine pollen in basal sediments

suggests that these cores are no more than 75 years old. Furthermore, Zn concentrations exceed ~30 μg g^{-1} in the upper 12–13 cm of the sediment column (31–39 μg g^{-1}), which is consistent with the fact that large-scale urbanisation of the adjacent Howick-Pakuranga catchments did not begin until the mid-1960's (Swales et al. 2002).

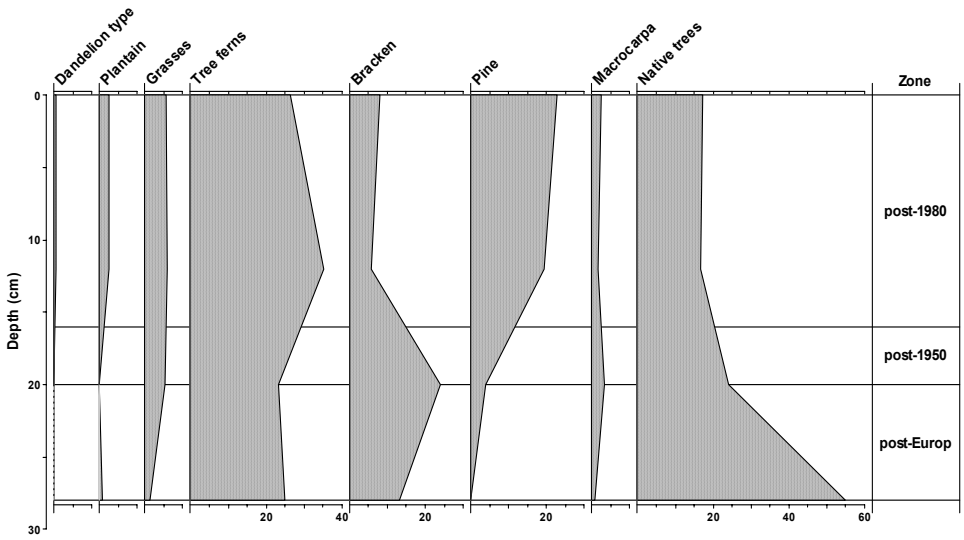

Figure 3.42: Whitford estuary sub-tidal core WH-S2 pollen and spore profiles for major plant groups expressed as percentage of terrestrial pollen and spore sum.

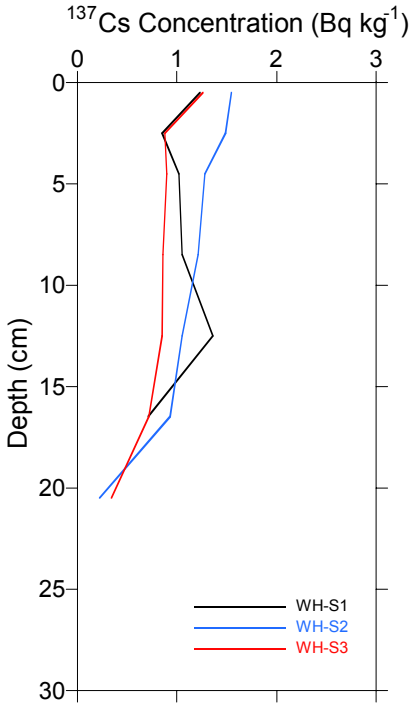

Figure 3.43: ^{137}Cs concentration profiles in the Whitford subtidal cores.

The ^{210}Pb profiles show substantial between-core variations in sedimentation and mixing in the subtidal sediments (Fig. 3.44). In core WH-S1, the ^{137}Cs SAR (3.8 mm yr^{-1}) is almost double the ^{210}Pb SAR (2.1 mm yr^{-1}), which may result from sediment mixing. The reduced ^{210}Pb concentration in the top 5 cm of the cores is indicative of an SML. If ^{137}Cs deposited in the early-1950's was rapidly mixed in the SML then the maximum depth of ^{137}Cs would be 13.5 cm, which yields a corrected ^{137}Cs SAR of 2.8 mm yr^{-1} that is similar to the ^{210}Pb SAR. This reasoning assumes a time-invariant SML of constant depth.

The ^{210}Pb profile in WH-S2 shows a constant ^{210}Pb concentration in the top 12.5 cm of the core and indicates deep mixing of sediments. This is consistent with the uniform pollen counts in this layer (Fig. 3.42). Unsurprisingly, there is a large difference between ^{210}Pb (0.6 mm yr^{-1}) and ^{137}Cs SAR (4.6 mm yr^{-1}). Correcting the ^{137}Cs SAR for the 12.5-cm SML (as above) yields a ^{137}Cs SAR (2.0 mm yr^{-1}) that is still ~3 times larger than the ^{210}Pb value.

Core WH-S3 displays a complex ^{210}Pb profile (Fig. 3.44) that is similar to core MH-I1 collected in the Mahurangi estuary (section 3.2.3), with a two-layer exponential decay

profile. In the top layer, which extends to 17 cm depth, the ^{210}Pb SAR is 5.7 mm yr^{-1} whereas the SAR in the bottom layer is only 1.6 mm yr^{-1}. The ^{137}Cs-derived SAR is 4.6 mm yr^{-1}.

This type of ^{210}Pb profile could result from deep mixing of the sediment column by benthic fauna. The benthic infauna in these subtidal sediments are dominated by the polychaete *Aotearia sulcaticeps* and the crab *Macrophthalmus hirtipes* (Lundquist et al. 2003). *Aotearia* is typically found in the top 5 cm of the sediment column whereas *Macrophthalmus* builds burrows, so that deep sediment mixing may occur. Alternatively, the observed ^{210}Pb profile may reflect a local change in the balance between sediment deposition and re-suspension resulting in increased SAR. Increased sediment delivery to the embayment is not a likely explanation because we do not see the same pattern in cores WH-S1 and WH-S2.

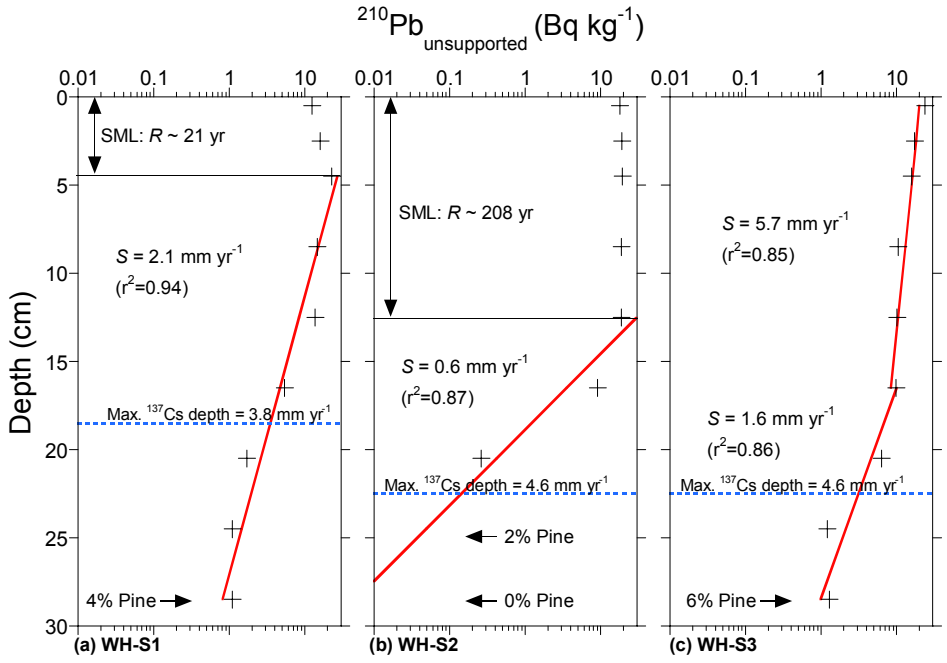

Figure 3.44: Whitford subtidal cores. Unsupported ^{210}Pb profiles plotted on a log scale, with linear regression fits used to calculate sedimentation rates (*S*). Also shown are the surface-mixed layer (SML), associated particle residence time (*R*) and the maximum depth of ^{137}Cs and average SAR.

The pollen profiles suggest that SAR have increased at least two-fold between the 1950–1980 (1.3–4.0 mm yr^{-1}) and post–1980 (4.8–7.6 mm yr^{-1}) periods (Fig. 3.45). The ^{210}Pb profile in core WH-S2 shows that the apparent increase in pollen-derived SAR after 1980 of 7.6 mm yr^{-1} is an artefact of sediment mixing (Fig. 3.44) rather than a local increase in sedimentation. Average sedimentation rates for the post-1950/1953 period derived from pollen and ^{137}Cs dating are similar, whereas the ^{210}Pb-derived SAR's are substantially lower. The presence of SML in the ^{210}Pb profiles provides evidence that recent pollen and ^{137}Cs has been mixed down the profile thereby increasing the observed SAR. The mixing corrected ^{137}Cs SAR of 2–2.8 mm yr^{-1} for cores WH-S1 and WH-S2 are closer to the ^{210}Pb values.

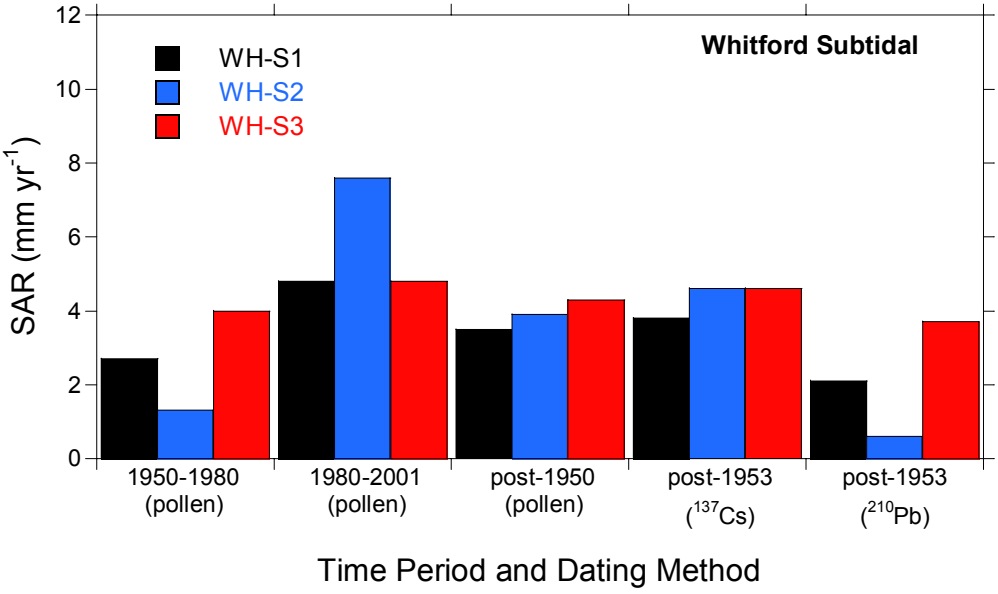

Figure 3.45: Whitford (sub-tidal), post-1950/1953 SAR estimated from pollen, ^{137}Cs and ^{210}Pb dating of sediment cores. The post 1953 ^{210}Pb SAR for core WH-S3 is an average of the values in the top and bottom layers (see Fig. 3.43).

3.8 Wairoa estuary (intertidal and sub-tidal cores)

3.8.1 Background

The Wairoa estuary is a mature, infilled, drowned-valley estuary fringing the southern shore of the Tamaki Strait (Fig. 3.46). The rapid "aging" of the estuary is unsurprising as its ~311 km^2 catchment is large in comparison to the estuary high-tide area

(i.e., ~3 km^2). Mangroves have almost completely colonised the intertidal flats on either side of the meandering main tidal channel (Fig. 3.47, Table 3.1). The infilled state of the estuary suggests that a substantial quantity of the annual catchment sediment load is likely to be exported from the estuary to the open coast. Some of this sediment is likely to be deposited on the shallow sub-tidal flats beyond the mouth of the Wairoa estuary.

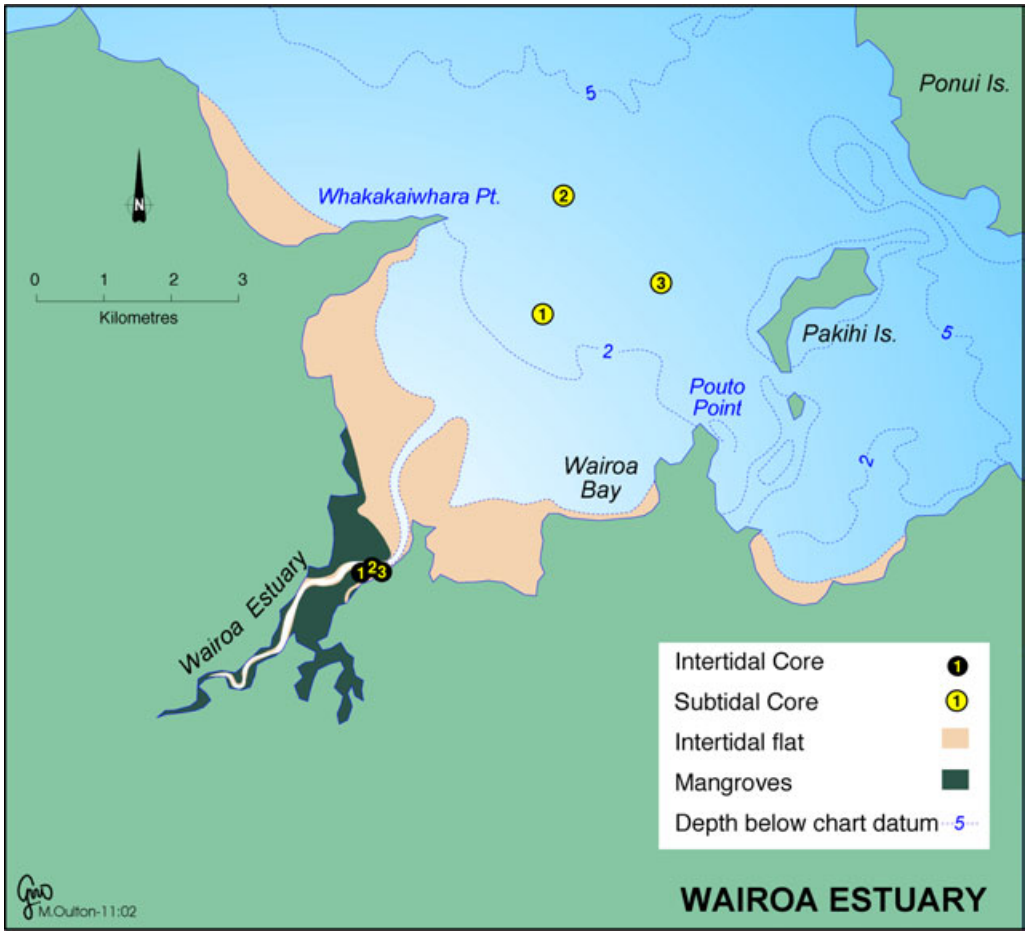

Figure 3.46: Wairoa estuary and embayment - location of sub-tidal and cores and major sub-environments.

Catchment deforestation began somewhat earlier than elsewhere in the Auckland region. Maori cultivated the flood plain along the estuary and traded with European whaling and sealing ships, which visited the Hauraki Gulf from the 1790's (Murdoch, 1988). Large-scale catchment deforestation followed European settlement, which began in 1852. Initially, forest was cleared from the flood plain and by 1944 pasture accounted for 45% of the catchment landcover. The Hunua ranges largely remained in native forest and scrub. Between 1944 and 1975 the proportion of pasture landcover increased to 64% (Tonkin and Taylor, 1996) and during this period the

Cosseys (1951–1954) and Wairoa (1972–1975) Dams were constructed. From 1975 to 1986 large areas of native forest and scrub in the Wairoa and Cosseys Dams sub-catchments were cleared and a ~1600 ha *P. radiata* forest established. Luckman et al. (1999) have estimated the annual soil loss from the Wairoa catchment under present-day landcover at ~17,500 tonnes yr^{-1}. Seventy percent of this soil is derived from pasture.

Figure 3.47: View of Wairoa estuary and embayment, looking north-west towards Duders Regional Park and Whakakaiwhara Point. Note that mangroves have almost completely colonized the intertidal flats.

3.8.2 Wairoa estuary sediments

Replicate sediment cores were collected from an intertidal mud flat in the lower estuary and from the sub-tidal flat (~2.5–4.0 m below CD) beyond the mouth of the Wairoa estuary (Fig. 3.45). The intertidal cores were taken ~100-m apart and parallel to the main tidal channel. The mud flat was deeply incised by numerous meandering drainage channels and covered with numerous crab burrows (Fig. 3.48). The sub-tidal cores were taken ~1.8 km apart in a triangular arrangement (Fig. 3.46). These cores contained shell valves of *Dosina zelandica*, *Austrovenus stutchburyi* (cockle), *sigapatella* sp., *Tellinota edgari* (Tellinid), *Maoriculpus roseus* (turret shell) and abundant oyster shell valves. These shellfish species are typically found in estuaries and sheltered coastal embayments, although *Dosina zelandica* does not usually occur in estuaries. Lundquist et al. (2003) found that the living benthic infauna are dominated by the polychaetes *Aotearia sulcaticeps* and *Labiosthenolepis laevis*, and the amphipod *Paracalliope novizealandiae*.

Intertidal sediments are muddy fine sands composed of fine silt (~20 μm modal diameter) and very fine sand (70–90 μm modal diameter). Sub-tidal sediments are also muddy fine sands, however the sand modal size is somewhat larger (110–140 μm modal diameter). The sub-tidal sediments also contained quantities of coarse sand-sized shell fragments. The depth profiles of dry bulk sediment density in the intertidal cores were all similar (range 0.6–0.9 g cm^{-3}), with a gradual increase in density with depth. The sub-tidal sediment density profiles were also similar but displayed a more

complex pattern than the intertidal cores. Here, dry bulk sediment density increased down core, with a high density layer (1.5–2.0 g cm^{-3}) coinciding with abundant shell fragments (Appendix IV).

Figure 3.48: Wairoa estuary, view of intertidal flat taken from core site WI-I3.

Profiles of D_{50} in the intertidal cores are almost identical (D_{50} range 50–70 μm), and display little variation with depth (Fig. 3.49a). In the sub-tidal cores the depth profiles for WA-S1 and WA-S3 are similar (D_{50} range 80–144 μm) whereas sediments in core WA-S2 are of substantially coarser texture (D_{50} range 400–800 μm) (Fig. 3.50a). Sediments in the intertidal cores are also generally muddier (mud content 40–60%) than the subtidal cores (mud content 5–40%) (Figs. 3.49b and 3.50b).

Zn concentration profiles in the intertidal cores are similar and show little variation with depth (range 31–45 μg g^{-1}) (Fig. 3.49c) and are higher than Zn concentrations in the sub-tidal cores (range 15–36 μg g^{-1}) (Fig. 3.50c). The data indicate that Zn concentrations in the Wairoa estuary intertidal sediments slightly exceed the range of pre-urbanised "background: values (i.e., 10–30 μg g^{-1}) for Auckland estuaries whereas Zn concentrations in sub-tidal sediments are within the range of natural variability.

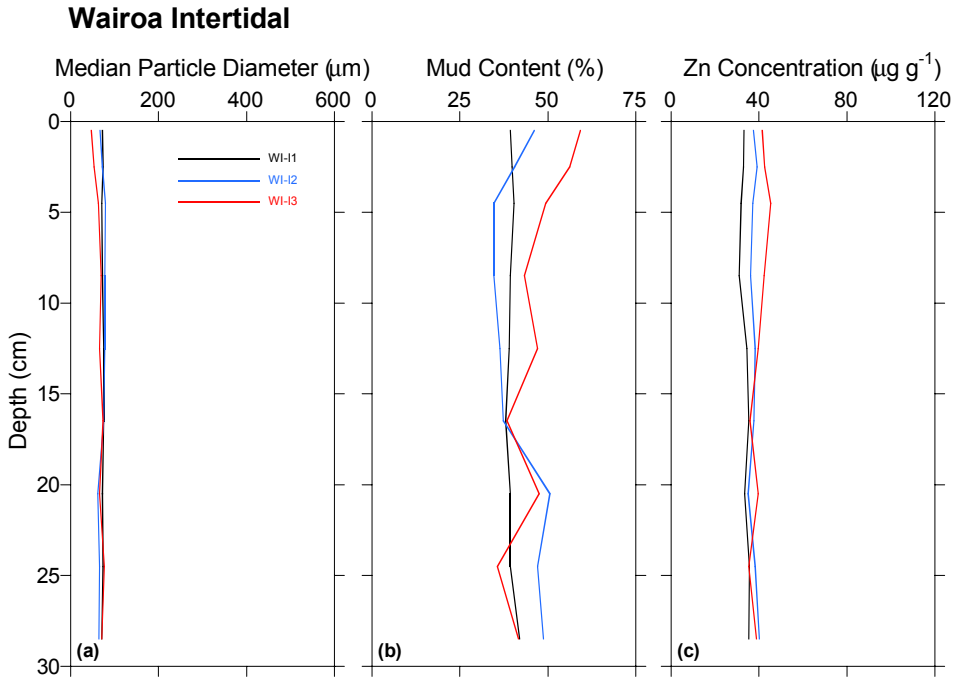

Figure 3.49: Wairoa intertidal cores (a) median particle diameter, (b) mud content and (c) Zn concentration profiles.

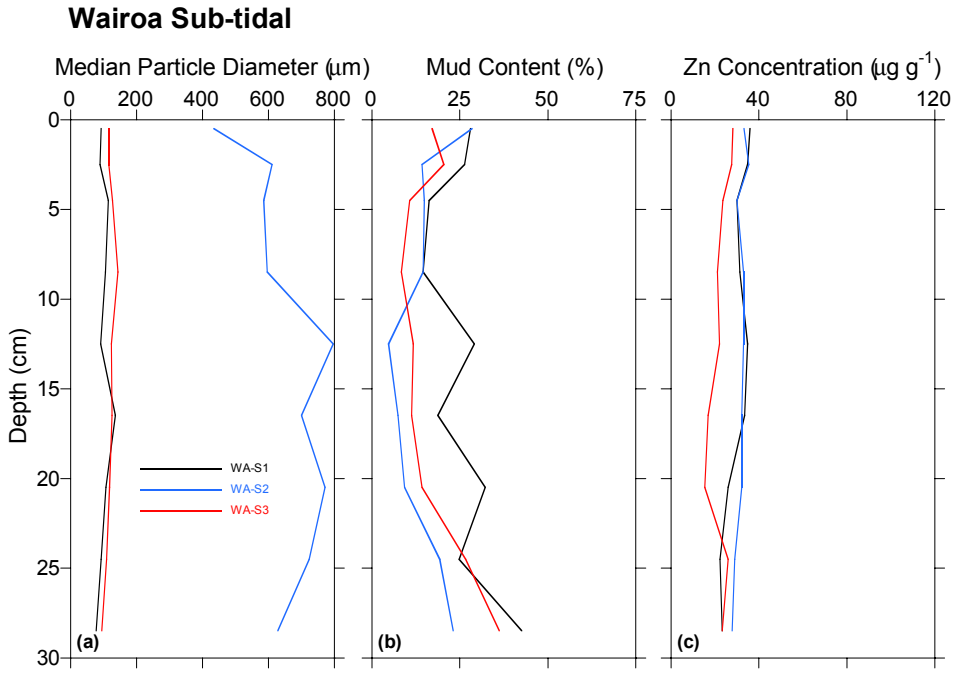

Figure 3.50: Wairoa sub-tidal cores (a) median particle diameter, (b) mud content and (c) Zn concentration profiles.

3.8.3 Wairoa recent sedimentation history

Intertidal cores

The pollen assemblages contained in the intertidal cores are similar to those preserved in the Puhoi estuary. The pollen content is dominated by tree-fern spores (50–65%), which is a strong indication that these sediments are derived from eroded catchment soils (Fig 3.51). The presence of pine pollen >5% of the total count at the base of the cores indicates that these sediments were deposited after 1950, which is consistent with the presence of ^{137}Cs to the bottom of each core (Fig. 3.52).

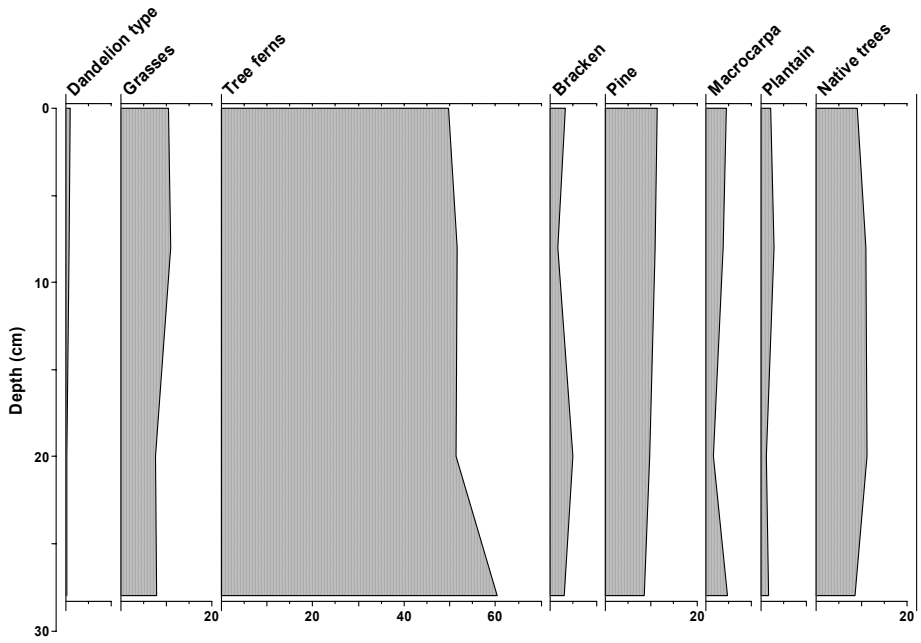

Figure 3.51: Wairoa estuary intertidal core WH-I2 pollen and spore profiles for major plant groups expressed as percentage of terrestrial pollen and spore sum.

The unsupported ^{210}Pb profiles for the Wairoa intertidal cores show only small reductions in concentrations (i.e., 20–35%) between the surface and 30-cm depth (Fig. 3.53). This pattern suggests that either (1) sedimentation has been very rapid or (2) deep sediment mixing has homogenised the profiles. In case (1), the 20-35% reduction in ^{210}Pb concentration between the top and bottom of the cores indicates that these sediments are younger than the ~22 year half-life of ^{210}Pb, with insufficient time since deposition for ^{210}Pb decay. The ^{210}Pb-derived SAR for cores WI-I2 (~27 mm yr^{-1}) and WI-I3 (~34 mm yr^{-1}) indicates that 30 cm of sediment have been deposited in the last ten years.

In case (2), physical mixing of sediments by waves or tidal currents is unlikely given that the site is sheltered from waves by its small fetch (i.e., < 100 m) and mangroves and the fact that tidal current speeds on intertidal flats rapidly reduce with distance from the channel. Migration of the small channels draining the intertidal would completely mix the sediment column to ~0.5-m depth, although we have no idea if migration occurs.

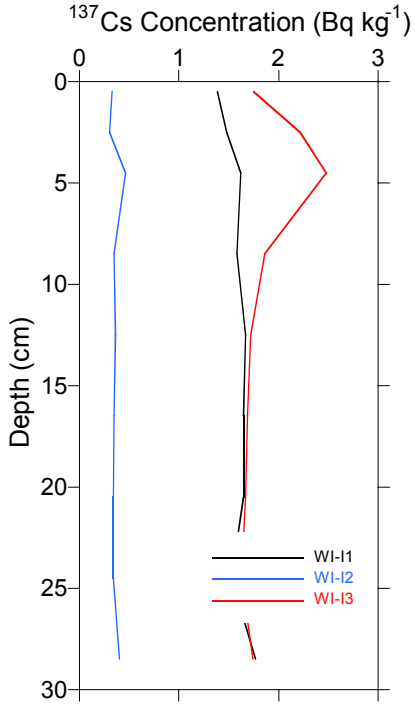

Figure 3.52: ^{137}Cs concentration profiles in the Wairoa intertidal cores.

The mud crab *Helice crassa* is the dominant fauna in these intertidal sediments (Lundquist et al. 2003), which are most abundant on mud flats at mean low water level. *H. crassa* typically burrows to ≤ 10 cm depth and the burrow volume can account for as much as 14% of the sediment column to ~10 cm depth (Morrisey et al. 1999b) and is likely to substantially bioturbate sediment within this layer. Given that *H. crassa* is restricted to the top 10 cm of the sediment column, then we would expect to see a surface mixed layer with a ^{210}Pb exponential decay profile below the SML. This does not occur and we conclude that the ^{210}Pb profiles primarily reflect rapid sedimentation rather than bioturbation.

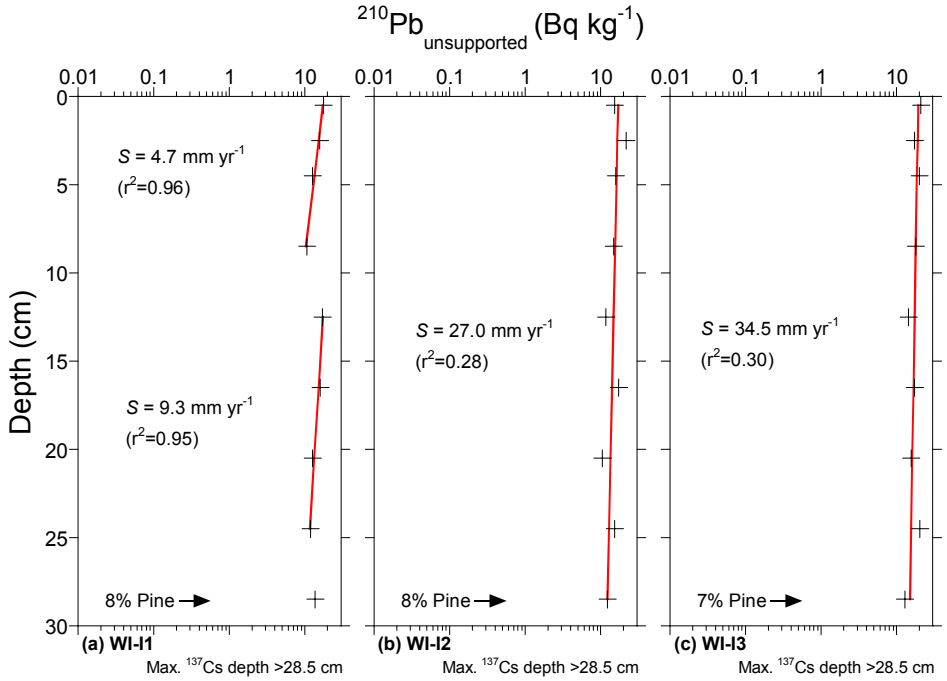

Figure 3.53: Wairoa intertidal cores. Unsupported ^{210}Pb profiles plotted on a log scale, with linear regression fits used to calculate sedimentation rates (*S*). Also shown is the maximum depth of ^{137}Cs and average SAR.

Sub-tidal cores

The occurrence of pine pollen in the bottom of the cores indicates that these sediments have been deposited since the mid-1930's (Fig. 3.54). The high proportion of tree fern spores (~40% of the pollen and spore total) in the cores likely reflects the fact that these sediments are derived from eroded catchment soils. The 1950 horizon in the cores occurs at 14-cm and 16-cm depth in cores WA-S1 and WA-S3 respectively, whereas this horizon is substantially deeper in core WA-S2 (22-cm depth). Pollen dating of post-1950 sediments is consistent with the ^{137}Cs profiles (Fig. 3.55), which also show a maximum depth (22.5 cm) occurring in core WA-S2.

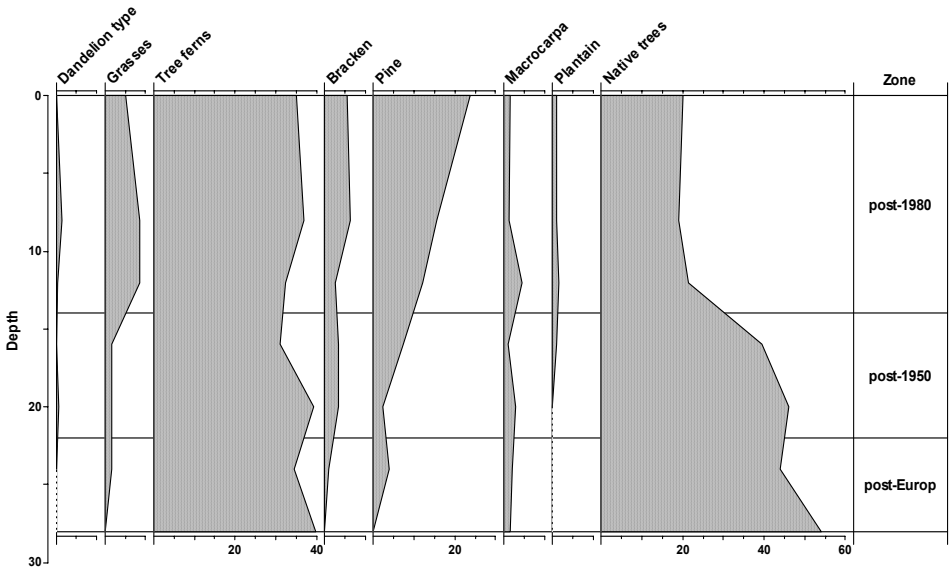

Figure 3.54: Wairoa estuary subtidal core WA-S2 pollen and spore profiles for major plant groups expressed as percentage of terrestrial pollen and spore sum.

The ^{210}Pb profiles for the Wairoa subtidal cores show a characteristic exponential decay with depth in the sediment column (Fig. 3.56). The similarity of the ^{210}Pb profiles between cores suggests that SAR in this area of the Tamaki Strait are spatially uniform. The ^{210}Pb-derived SAR of 3.3–4.3 mm yr^{-1} are similar to the ^{137}Cs-derived SAR (3.0–4.6 mm yr^{-1}) and pollen SAR (2.7–4.3 mm yr^{-1}) for the post-1953 period (Fig. 3.56). The pollen data also suggest a two-fold increase in SAR from 1.3–2.7 mm yr^{-1} (1950–1980) to 4.8–6.7 mm yr^{-1} since 1980 (Fig. 3.57).

The close agreement between the dating methods and good linear-regression fits to the ^{210}Pb data in the Wairoa subtidal cores enable detailed sedimentation histories to be developed for the last ~150 years using the constrained ^{210}Pb CRS dating model (Figs. 3.58–3.60). We calculate depth-age, age-mass sedimentation (g cm^{-2} yr^{-1}) and age-SAR (mm yr^{-1}) curves for three depth increments. This accounts for the uncertainty in the maximum depth of ^{137}Cs ($^{137}Cs_{max}$), which results from the 4-cm depth interval between samples.

For core WA-S1, results are only available for the $^{137}Cs_{max}$=16.5-cm case because there is insufficient unsupported ^{210}Pb in the profile below that depth to satisfy Equation 4. There is close agreement between the CRS and CIC model depth-age curves for sediments <50 years old (Fig. 3.58a), while the dating curves diverge for

older sediments. The age-mass sedimentation curves show a four-fold increase from ~0.1 g cm^{-2} yr^{-1} 150 years ago to ~0.4 g cm^{-2} yr^{-1} ~25 years ago and reducing to ~0.35 g cm^{-2} yr^{-1} today (Fig. 3.58b). Similarly, the age-SAR curves indicate that net sedimentation rates have increased from pre-deforestation values of ~0.5 mm yr^{-1} and increasing to ~4 mm yr^{-1} today (Fig. 3.58c).

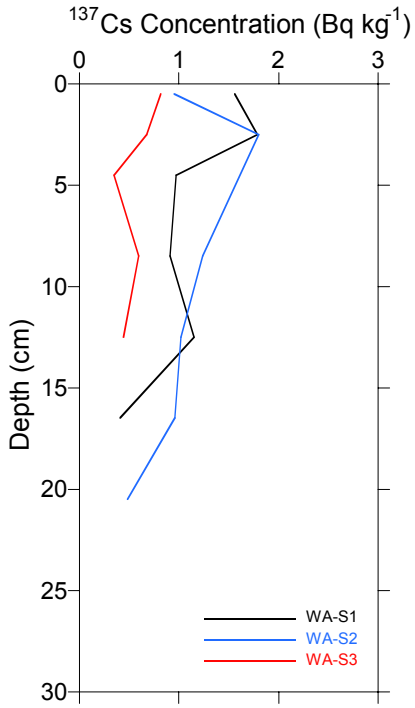

Figure 3.55: ^{137}Cs concentration profiles in the Wairoa subtidal cores.

Table 3.4 summarises the constrained ^{210}Pb CRS modelling results for core WA-S1. The mean supply rate (*P*) of 0.0075 Bq cm^{-2} yr^{-1} is similar to the 0.0059 Bq cm^{-2} yr^{-1} directly measured in rainwater during the 2002–2003 year. This similarity, along with the good agreement with pollen and ^{137}Cs SAR provides confidence in the sedimentation chronology reconstructed for core WA-S1.

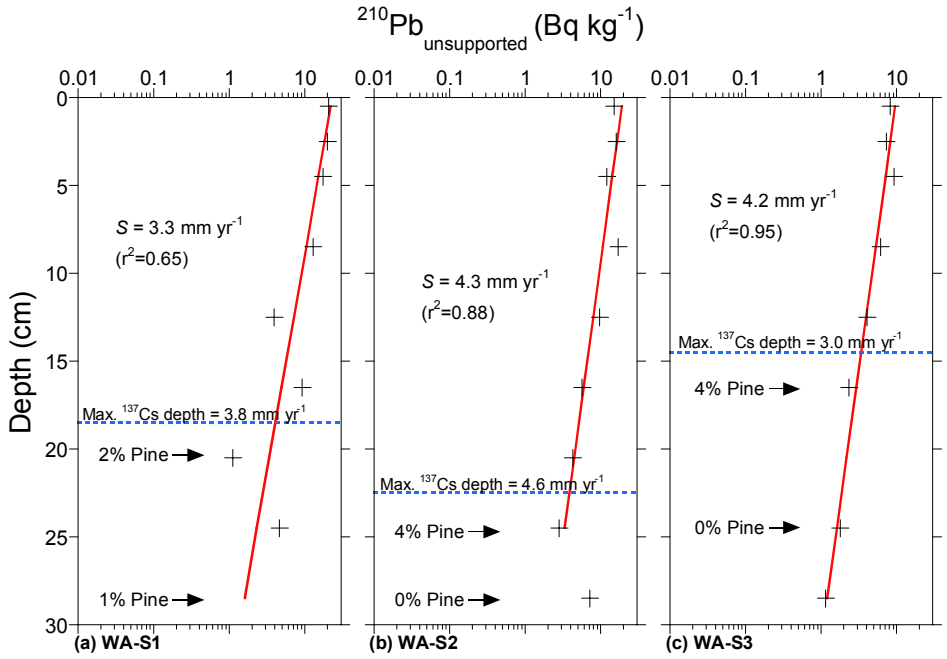

Figure 3.56: Wairoa subtidal cores. Unsupported ^{210}Pb profiles plotted on a log scale, with linear regression fits used to calculate sedimentation rates (*S*). Also shown is the maximum depth of ^{137}Cs and average SAR.

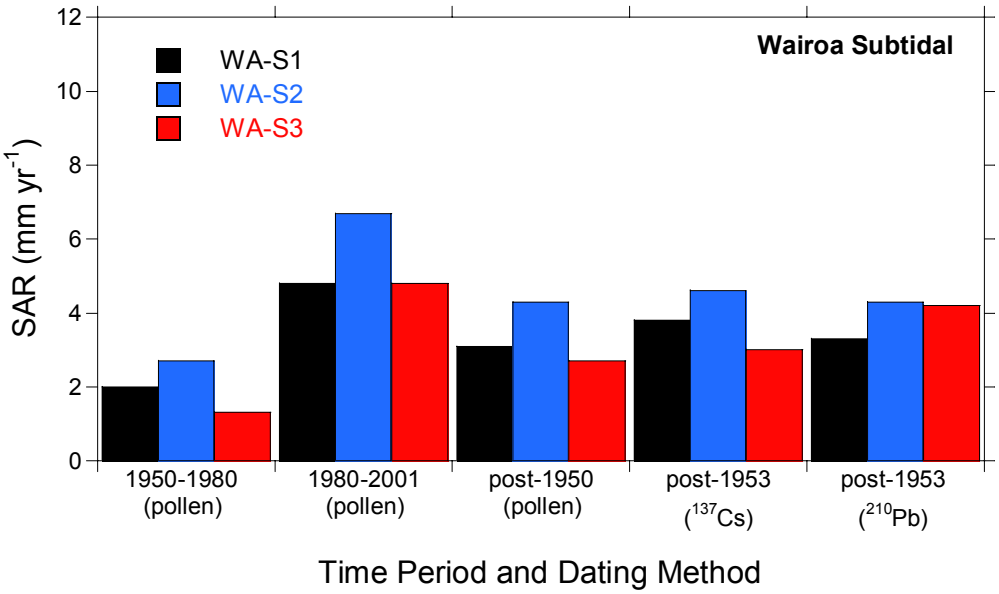

Figure 3.57: Wairoa subtidal cores, post-1950/1953 SAR estimated from pollen, ^{137}Cs and ^{210}Pb dating of sediment cores.

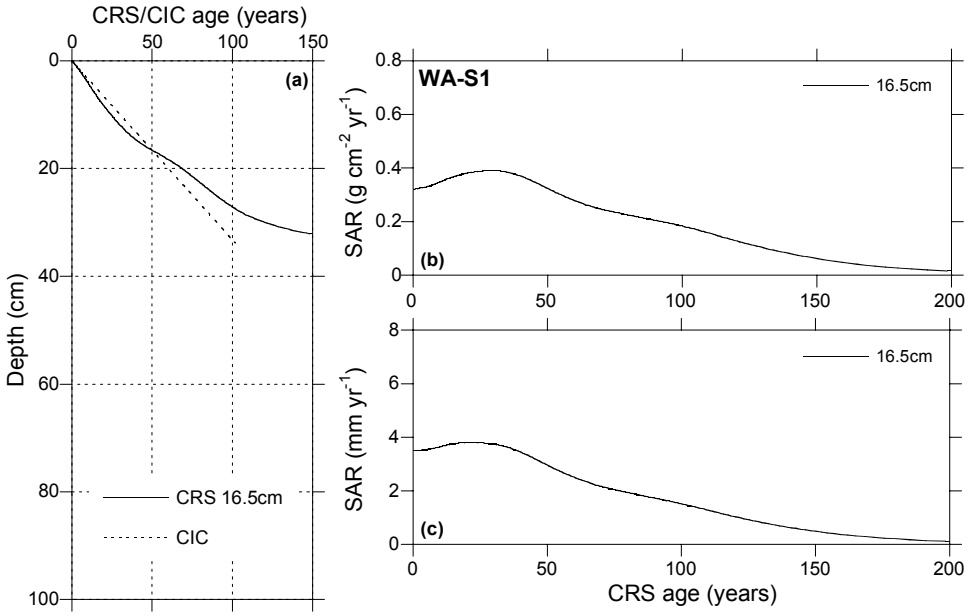

Figure 3.58: Core WA-S1 sedimentation chronology (a) depth-age curves for CRS and CIC ^{210}Pb models, (b) age-mass (g cm^{-2} yr^{-1}) accumulation curves and (c) age-SAR (mm yr^{-1}) curves based on the constrained CRS model.

Table 3.4: Summary of constrained ^{210}Pb CRS modelling results for core WA-S1: linear regression fit to natural-log transformed ^{210}Pb data; depth for integration of ^{210}Pb profile; total unsupported ^{210}Pb in the profile ($A(o)$) and mean annual flux (P).

	$^{137}Cs_{max}$ = 20.5 cm
^{210}Pb profile fit (r^2)	0.65
^{210}Pb profile depth (cm)	33.9
***A*(*o*)** (Bq cm^{-2})	0.2392
P (Bq cm^{-2} yr^{-1})	0.0075

The depth-age curves for core WA-S2 show good agreement between the CRS and CIC dating models for the last 100 years (Fig. 3.59a). The age-mass sedimentation curves for the 20.5-cm and 22.5-cm ^{137}Cs maximum depth cases show a four-fold increase from ~0.1 g cm^{-2} yr^{-1} 150 years ago to ~0.4 g cm^{-2} yr^{-1} to the present today (Fig. 3.59b). The age-SAR curves indicate that SAR increased from pre-deforestation values of <1 mm yr^{-1} and increasing to ~5.5 mm yr^{-1} today (Fig. 3.59c). The age-mass and age-SAR curves for the 24.5cm case diverge markedly from the other two cases, which indicates that there is insufficient unsupported ^{210}Pb at depth to obtain a

reliable result. This is also shown by the large increase in depth between the 22.5-cm and 24.5-cm cases required to satisfy Equation 4 (Table 3.5).

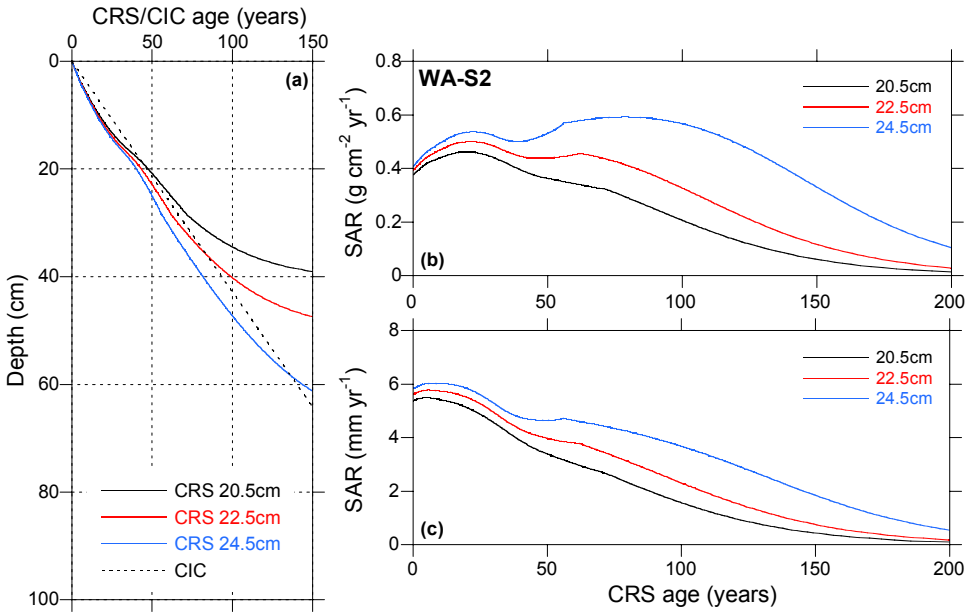

Figure 3.59: Core WA-S2 sedimentation chronology (a) depth-age curves for CRS and CIC ^{210}Pb models, (b) age-mass (g cm^{-2} yr^{-1}) accumulation curves and (c) age-SAR (mm yr^{-1}) curves based on the constrained CRS model.

Table 3.5: Summary of constrained ^{210}Pb CRS modelling results for core WA-S2: linear regression fit to natural-log transformed ^{210}Pb data; depth for integration of ^{210}Pb profile; total unsupported ^{210}Pb in the profile ($A(o)$) and mean annual flux (P).

	$^{137}Cs_{max}$ = 20.5 cm	$^{137}Cs_{max}$ = 22.5 cm	$^{137}Cs_{max}$ = 24.5 cm
^{210}Pb profile fit (r^2)	0.88	–	–
^{210}Pb profile depth (cm)	40.5	50.1	68.7
***A*(*o*)** (Bq cm^{-2})	0.2393	0.2497	0.2587
P (Bq cm^{-2} yr^{-1})	0.0075	0.0078	0.0081

Table 3.5 summarises the constrained ^{210}Pb CRS modelling results for core WA-S2. The range of mean supply rates (P) of 0.0075–0.0078 Bq cm^{-2} yr^{-1} (20.5-cm and 22.5-cm cases) are similar to the 0.0075 Bq cm^{-2} yr^{-1} obtained for WA-S1 and the measured atmospheric flux (0.0059 Bq cm^{-2} yr^{-1}). These results are consistent with the

assumptions of the CRS model and provide confidence in the sedimentation chronology reconstructed for cores WA-S1 and WA-S2.

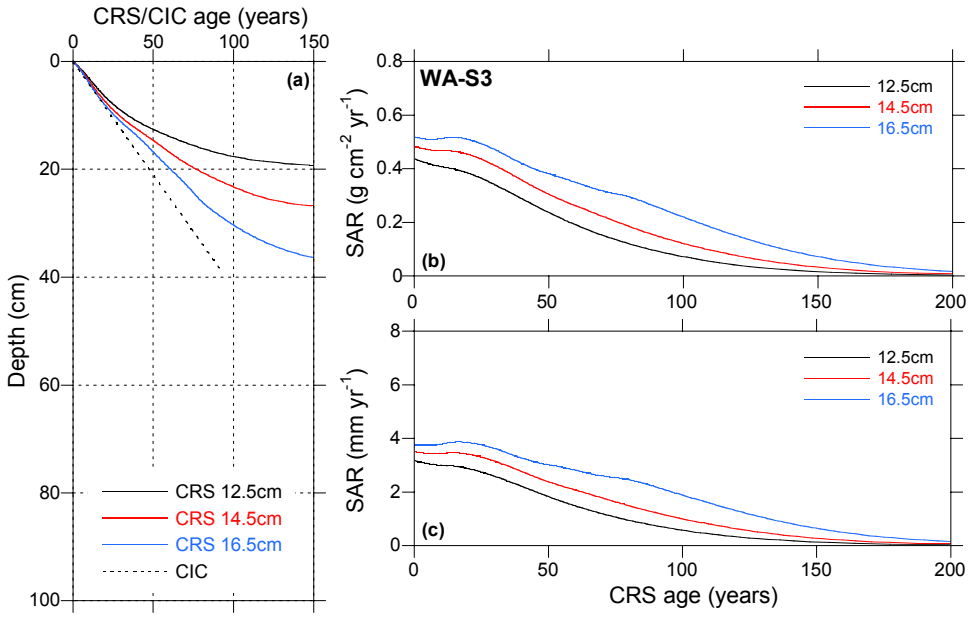

Figure 3.60: Core WA-S3 sedimentation chronology (a) depth-age curves for CRS and CIC ^{210}Pb models, (b) age-mass (g cm^{-2} yr^{-1}) accumulation curves and (c) age-SAR (mm yr^{-1}) curves based on the constrained CRS model.

The CRS and CIC depth-age curves for core WA-S3 diverge markedly below 10cm depth (Fig. 3.60a), which can be expected when sedimentation rates have increased (Blais et al. 1995). The age-mass sedimentation curves show an increase from ~0.1 g cm^{-2} yr^{-1} 150 years ago to ~0.5 g cm^{-2} yr^{-1} today (Fig. 3.60b). The age-SAR curves indicate that SAR increased from pre-deforestation values of ~0.5 mm yr^{-1} to ~3.5 mm yr^{-1} today (Fig. 3.60c). Table 3.6 summarises the constrained ^{210}Pb CRS modelling results for core WA-S3. The range of mean supply rates (*P*) of 0.0044–0.0052 Bq cm^{-2} yr^{-1} are ~40% less than for cores WA-S1 and WA-S2 (0.0075–0.0078 Bq cm^{-2} yr^{-1}) although similar to the measured atmospheric flux (0.0059 Bq cm^{-2} yr^{-1}).

Table 3.6: Summary of constrained ^{210}Pb CRS modelling results for core WA-S3: linear regression fit to natural-log transformed ^{210}Pb data; depth for integration of ^{210}Pb profile; total unsupported ^{210}Pb in the profile ($A(o)$) and mean annual flux (P).

	$^{137}Cs_{max}$ = 12.5 cm	$^{137}Cs_{max}$ = 14.5 cm	$^{137}Cs_{max}$ = 16.5 cm
^{210}Pb profile fit (r^2)	0.95	–	–
^{210}Pb profile depth (cm)	19.7	27.8	38.7
***A*(*o*)** (Bq cm^{-2})	0.1404	0.1558	0.1663
P (Bq cm^{-2} yr^{-1})	0.0044	0.0049	0.0052

3.9 Te Matuku estuary (intertidal cores)

3.9.1 Background

Te Matuku estuary is a small (~2 km^2) coastal embayment (Table 3.1), which opens to the sea on the southern shore of Waiheke Island and 11 km north of the Wairoa estuary mouth (Fig. 3.61). The estuary is deeply indented into the surrounding terrain, which is up to 100 m above mean sea level. The estuary has largely infilled so that the main tidal channel is also intertidal. The upper estuary is also fringed by extensive stands of mangrove. Because the estuary is largely intertidal, there is almost complete exchange of estuarine water with each tidal cycle. The estuary receives runoff from a 12.2-km^2 catchment.

The original landcover of Waiheke Island was a mixed podocarp-kauri forest, which was dominated by tawa, rimu and kauri, while totara and matai were rare. Taraire, red beech, pohutakawa and puriri were common along the coastal margin (Monin, 1992). Maori agricultural practices resulted in the removal of forest areas by fire and cultivation for several years before repeating the cycle elsewhere (Monin, 1992). In 1878 the botanist Thomas Kirk recorded that kauri was still common at the eastern end of Waiheke Island. Large areas of kanuka forest noted by Kirk are indicative of the earlier loss of podocarp-kauri forest, most likely by fire. Europeans settled Te Matuku from the mid-1850's. Robert McLeod established a public house in 1855 and began logging trees from his 777-acre holding on the peninsula separating Te Matuku and Awaawaroa bays whereas John and Mary Fraser arrived in 1860 to farm 220 acres at Te Matuku (Monin, 1992). By the 1920's large areas of the catchment had been converted to pasture.

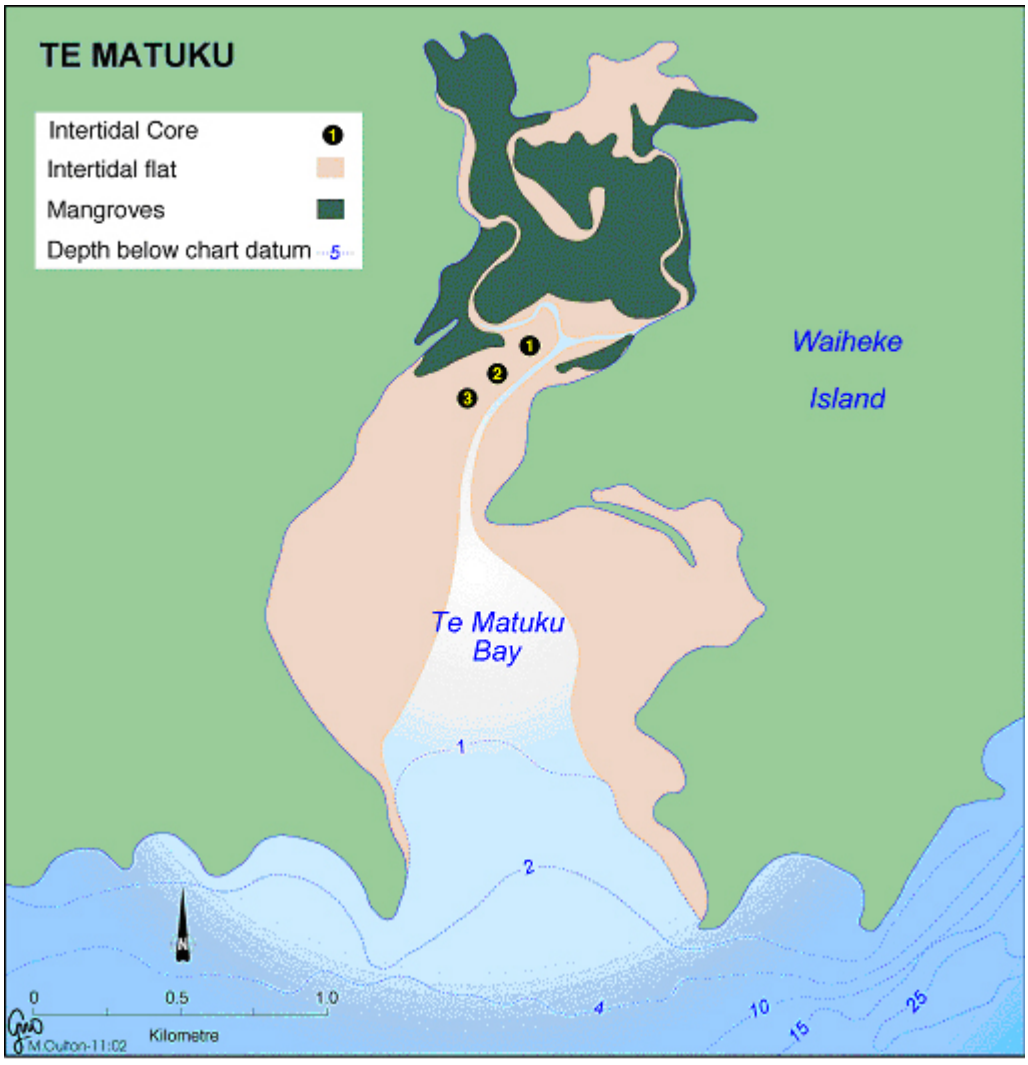

Figure 3.61: Te Matuku embayment - location of sub-tidal and cores and major sub-environments.

The McLeod family were grazing several thousand ewes on their property at this time (Mr Rob Fenwick, pers. comm. September 2003). A series of aerial photographs (1940–2002) show that the Te Matuku peninsula began to revert to scrub from 1940, which suggests that stock grazing had been abandoned by the late 1930's. Present day catchment landcover is comprised of regenerating native forest (36%), scrub (15%) and pasture (49%) (source: NZ Land Resource Inventory).

3.9.2 Te Matuku sediments

Sediment cores were taken on the mid-intertidal flat parallel to the main channel and ~150 m apart (Fig. 3.61). Sediments are typically muddy fine sands composed of fine silt (~20 μm modal diameter) and very fine sand (~100–150 μm modal diameter). Dry

bulk sediment density profiles are similar in all cores (Appendix IV) and increase from ~1.1 g cm^{-3}) in surface sediments to ~1.4 g cm^{-3} at the base of each core.

Profiles of D_{50} show negligible variation with depth (D_{50} range = 100–180 µm), although particle size appears to decrease towards the estuary mouth (Fig. 3.62a). Furthermore, the mud content of sediments also increases towards the estuary mouth in the top-most 15-cm of the cores from ~10–20% (TM-I1) to ~25–37% (TM-I3) (Fig. 3.62b).

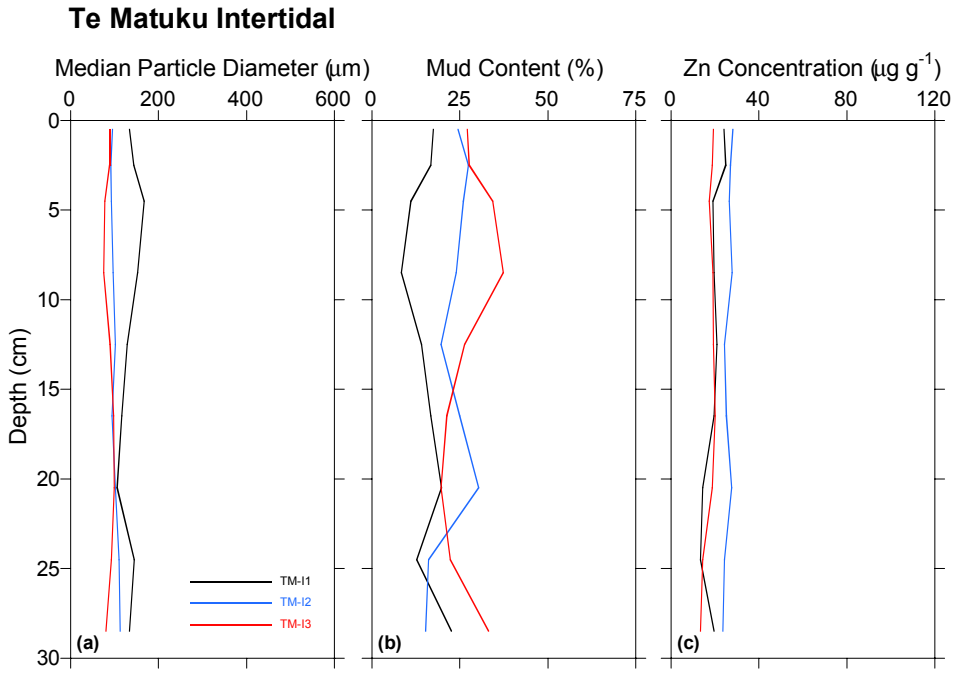

Figure 3.62: Te Matuku intertidal cores (a) median particle diameter, (b) mud content and (c) Zn concentration profiles.

The Zn concentration profiles show only small increases with decreasing depth (maximum ~5 µg g^{-1}) (Fig. 3.62c) and are within the range of pre-urban "background" values (i.e., 10–30 µg g^{-1}) observed in Auckland estuaries.

3.9.3 Te Matuku recent sedimentation history

The estuarine sediments have preserved an excellent pollen record in Te Matuku bay. In core TM-I1, the absence of bracken, in coincidence with the occurrence of native tree pollen, suggests that sediments below 24-cm depth were deposited during the (pre-1840) Maori period (Fig. 3.63). Sampling of Maori-period sediments near the base of core TM-I1 enables a tentative estimate of sedimentation during the post-

European (1840–1950 A.D.) period to be made. The average sedimentation rate for the 1840–1950 A.D. period is ~0.6 mm yr^{-1}.

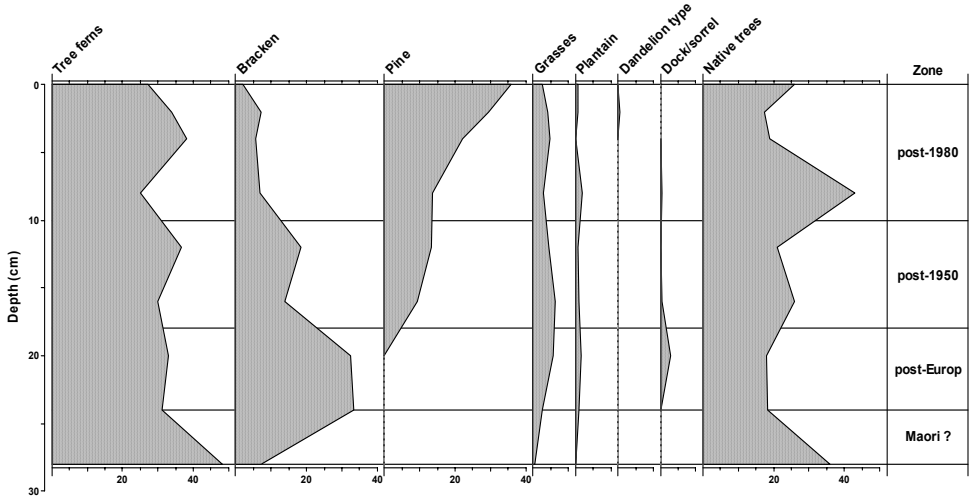

Figure 3.63: Te Matuku embayment intertidal core TM-I1 pollen and spore profiles for major plant groups expressed as percentage of terrestrial pollen and spore sum.

The emergence of pine pollen at 20-cm depth in core TM-I1 and at 28-cm depth in core TM-I3 clearly identifies the post-1950 period. The presence of pine pollen at ~5% of the total pollen and spore count in TM-I2 basal sediments clearly shows that this core preserves a record of more rapid sedimentation (Appendix II).

The ^{137}Cs profiles (Fig. 3.64) are generally consistent with the pollen-derived 1950 depth horizon although in cores TM-I1 and TM-I3 the maximum depth of ^{137}Cs (1953) is as much as 4-cm below the 1950 pollen layer. These differences are within the combined uncertainty of assigning ages to the sediment layers, primarily because of the 4-cm depth interval between samples. The deeper ^{137}Cs profile in core TM-I2 is entirely consistent with the relatively higher sedimentation rate at this site implied by the pollen profiles.

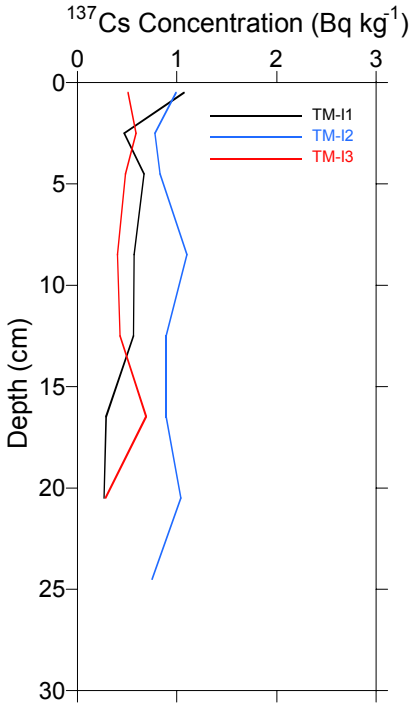

Figure 3.64: ^{137}Cs concentration profiles in the Te Matuku intertidal cores.

The ^{210}Pb profiles for the Te Matuku intertidal cores are similar to the nearby Wairoa subtidal cores (Fig. 3.56) in that they show a characteristic exponential decay with depth in the sediment. The ^{210}Pb-derived SAR of 4.2–8.7 mm yr^{-1} decline towards the mouth of the bay and are somewhat higher than the ^{137}Cs-derived SAR (4.6–5.4 mm yr^{-1}) and pollen SAR (3.5–5.1 mm yr^{-1}) for the post 1950/1953 period (Fig. 3.66). The pollen data suggest that sedimentation rates in Te Matuku Bay have substantially increased since 1980 (Fig. 3.66). Sedimentation rates during the 1950–1980 period averaged 1.3 mm yr^{-1} in cores TM-I2 and TM-I3 and 2.7 mm yr^{-1} near the catchment outlet (TM-I1). Since 1980, sedimentation rates in Te Matuku Bay have averaged 4.8–10.5 mm yr^{-1}, which in cores TM-I2 and TM-I3 represents a 7–8-fold increase.